Benefits of Range-Separated Hybrid and Double-Hybrid Functionals for a Large and Diverse Data Set of Reaction Energies and Barrier Heights

Published as part of The Journal of Physical Chemistry virtual special issue "Vincenzo Barone Festschrift".

Golokesh Santra, Rivka Calinsky, and Jan M. L. Martin*

ACCESS | Metrics & More | Article Recommendations | SI Supporting Information

ABSTRACT: To better understand the thermochemical kinetics and mechanism of a specific chemical reaction, an accurate estimation of barrier heights (forward and reverse) and reaction energies is vital. Because of the large size of reactants and transition state structures involved in real-life mechanistic studies (e.g., enzymatically catalyzed reactions), density functional theory remains the workhorse for such calculations. In this paper, we have assessed the performance of 91 density functionals for modeling the reaction energies and barrier heights on a large and chemically diverse data set (BH9) composed of 449 organic chemistry reactions. We have shown that range-separated hybrid functionals perform better than the global hybrids for BH9 barrier heights and reaction energies. Except for the PBE-based range-separated nonempirical double hybrids, range separation of the exchange term helps improve the performance for barrier heights and reaction energies. The 16-parameter Berkeley double hybrid, ωB97M(2), performs remarkably well for both properties. However, our minimally empirical range-separated double hybrid functionals offer marginally better accuracy than ωB97M(2) for BH9 barrier heights and reaction energies.
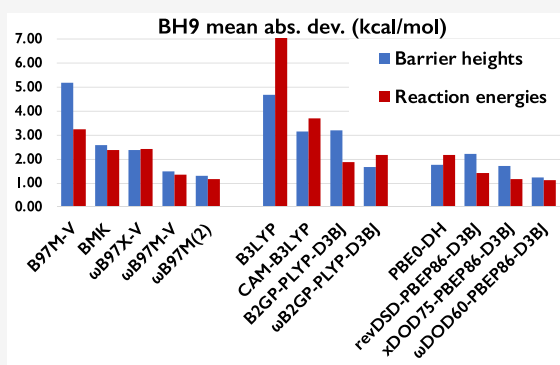
1. INTRODUCTION

Accurate predictions of kinetic and thermochemical properties are crucial for understanding the mechanisms of different chemical reactions involving main group elements, transition metals, and enzymes.[1,2] By definition, the reaction energy (RE) is the energy difference between the product(s) and reactant(s) in their equilibrium state, which has a direct influence on the equilibrium constant of a reaction. On the other hand, barrier heights (BH) are the energy differences between the product(s) or reactant(s) with the transition state (TS). The forward and reverse BHs are the determining components of the reversibility of a reaction.

Traditionally, 1 kcal/mol is considered "chemical accuracy" for bond dissociation energies, heats of reaction, activation barriers, etc. However, a change of approximately 1.4 kcal/mol in free energy at room temperature results in a difference of an order of magnitude for equilibrium constants and reaction rate.[2] Hence, one might choose 1.4 kcal/mol as a "chemical accuracy" criterion for BHs and REs. Highly accurate composite wave function *ab initio* methods (for reviews, see refs 3−8) can readily achieve this accuracy, but (at least for canonical approaches) their steep computational cost scaling with system size precludes their application to large molecules. As a result, Kohn−Sham density functional theory (KS-DFT[9]) is often seen as the "bread

and butter" alternative for calculations involving large organic molecules and enzymes.

Depending on the kinds of information employed in the exchange-correlation (XC) functional, Perdew[10] organized DFT methods into what he called a "Jacob's Ladder". On each rung of that ladder, dependence on a new type of information is introduced in the XC functional: the density itself on rung 1 (LDA), the reduced density gradient on rung 2 (GGAs), higher density derivatives or the kinetic energy density on rung 3 (meta-GGAs), occupied orbitals on rung 4, and unoccupied orbitals on rung 5. So-called hybrid and double-hybrid functionals belong to rungs 4 and 5, respectively. In the long-distance limit, the exchange potential of global hybrids deviates from its correct $-1/r_{12}$ form (r_{12} being the interelectronic distance).[11] Hence, to restore this behavior, the Coulomb operator is partitioned into a short-range (SR) component to be treated by a (meta)GGA, and a long-range (LR) component to
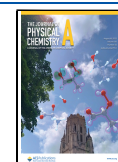
be treated by exact exchange, and one "crossfades" from SR to LR using an error function of r_{12}. According to Handy and co-workers,[11] the equation has the form:

$$\frac{1}{r_{12}} = \underbrace{\frac{1-[\alpha+\beta\mathrm{erf}(\omega r_{12})]/r_{12}}{}}_{\mathrm{SR=Short\text{-}Range}} + \underbrace{\frac{\alpha+\beta\mathrm{erf}(\omega r_{12})/r_{12}}{}}_{\mathrm{LR=Long\text{-}Range}}$$

where the range separation parameter (ω) can either be determined empirically using a training set[11-16] or by minimizing the deviation from the conditions the exact KS functional must obey.[17,18] The parameter α represents the percentage of HF exchange in the short-range limit, and $\alpha+\beta$ is the corresponding percentage in the long-range limit.

Over the years, several empirical and nonempirical range-separated hybrid (RSH) functionals following the above scheme have been proposed such as LC-ωPBE,[19] M11,[15] CAM-B3LYP,[11] ωB97X-V,[20] ωB97M-V,[21] and many more. Climbing up one step on the ladder, Ángyán and co-workers[22] and the Head-Gordon group[23] suggested adding a range-separated GLPT2 (second-order Görling–Levy perturbation theory[24]) correction term upon the RSH scheme for accurate long-range correlation energies. However, for their combinatorially optimized, range-separated double hybrid, ωB97M(2),[25] Mardirossian and Head-Gordon instead obtained orbitals from an RSH calculation and then evaluated the GLPT2 correlation in the basis of these orbitals. (ωB97M(2) uses same full semilocal correlation in the orbital generation step as does XYG3[26] and the xDSD functionals considered below. For detailed discussion on DH vs xDH, and on MP2 vs GLPT2 correlation, see refs 27 and 28, respectively.) Goerigk and co-workers[29-31] and Mester and Kállay[32-35] also proposed and benchmarked several range-separated double hybrid (RSDH) functionals, mainly for the electronic excitation energies. For our range-separated dispersion-corrected spin component scaled double hybrids (ωDSD),[36] we used KS orbitals from a standard global hybrid with full semilocal correlation to evaluate the PT2 energies. Adamo et al.[37] combined their 'nonempirical' quadratic integrated double hybrid (QIDH)[38] model with Savin's[39] RSX (range-separated exchange) scheme to propose RSX-QIDH. The range-separation parameter for the RSX-double hybrids was fitted to the exact total ground-state energy of the hydrogen atom. Following the idea of the RSH+MP2[22] method, Kalai and Toulouse[40] proposed a general scheme for RSDHs, where they recommended using range-separation for both exchange and PT2 correlation terms. Recently, Prokopiou et al.[41] have developed an optimally tuned RSDH functional by substituting the degeneracy-corrected perturbation theory (DCPT2[42]) for GLPT2. (We note in passing that the analytical first[43] and second[44] derivatives for DHs are available in the literature, not just in the gas phase but also in continuum solvents.[45] This is of interest not merely for computational spectroscopy, see refs 46 and 47 and references therein, but also will greatly facilitate locating accurate transition state structures.)

Several benchmark studies have shown excellent performance of range-separated hybrid and double hybrid functionals for calculating the barrier heights and reaction energies involving small- and medium-size organic molecules,[36,48-53] transition metals,[36,54-57] and enzymatically catalyzed reactions.[58,59] However, most barrier height and reaction energy data sets available in the literature either focus on only one specific type of reaction, or involve reactant and product molecules that are not large enough to represent the systems typically encountered in mechanistic studies.[58,60-68] Hence, assessing quantum chemical

methods on kinetic and thermochemical properties based on such databases is prone to bias. Aiming to solve this issue, DiLabio and co-workers[69,70] have recently proposed a large and sufficiently diverse benchmark set, BH9, composed of 449 reaction energies and 898 barrier heights (including forward and reverse). Their data set contains nine types of reactions: (i) radical rearrangement, (ii) Diels–Alder, (iii) halogen atom transfer, (iv) hydrogen atom transfer, (v) hydride transfer, (vi) B- and Si-containing reactions, (vii) proton transfer, (viii) nucleophilic substitution, and (ix) nucleophilic addition. The reference energies were computed at the DLPNO−CCSD-(T)[71-75] (domain-based local pair natural orbital coupled-cluster singles and doubles plus quasiperturbative triples) level of theory at the complete basis set limit.

In ref 70, the authors assessed the performance of 25 functionals on the first four rungs of the Jacob's Ladder. Other than that, a benchmark study of 18 double hybrid functionals using a reduced version (15 reactions were removed) of BH9 has recently been published by Brémond et al.[76] Interestingly, for both BH and RE, a lower-rung RSH functional, ωB97M-V, outperformed the best performing double hybrids recommended in ref 76. On top of that, the authors of ref 76 considered only a handful of RSDHs, which did not perform well in previous benchmark studies.[36,50,51] Hence, the main objective of the present study is to assess the performance of a variety of range-separated hybrid and double hybrid functionals on BH9 to verify whether range separation is superior to the global variants throughout. Alongside, we shall explore the effect of systematically increasing the fraction of HF exchange on the performance of global hybrid functionals.

2. COMPUTATIONAL DETAILS

All electronic structure calculations have been performed with ORCA 5.0.3[77] and QChem 5.4.2[78] running on the Faculty of Chemistry HPC facility. Except for the nucleophilic substitution reactions (i.e., Subset VIII), the Weigend−Ahlrichs family def2-QZVPP[79] basis set has been used throughout. As the reactions of subset VIII contain anions other than hydrides, we have used the minimally augmented diffuse basis set, ma-def2-QZVPP,[80] instead. Appropriate RI[81] basis sets are also employed for the correlation energies. For the ORCA calculations, DEFGRID3 and the RIJCOSX (resolution of the identity in combination with the chain of spheres[82] algorithm) approximations have been used. A pruned integration grid, SG-3,[83] is utilized for the QChem calculations. We have considered 91 functionals for the present study ranging from pure GGA (or meta GGA) to range-separated double hybrids. Depending on the exchange and correlation combination used for constructing the functionals, we have divided these 91 functionals into four categories: B97-family, PBE$_x$-PBE$_c$-based, B88-LYP-based, and PBE-P86-based. For the B97−V family functionals, the nonlocal VV10 correction was added in the post-SCF form.

The performance of these functionals is evaluated using the mean absolute deviation (MAD) calculated with respect to the DLPNO−CCSD(T)/CBS reference BHs and REs extracted from ref 70. See Tables S2−S5 in the Supporting Information for the corresponding root−mean−square deviations (RMSD), mean signed deviations (MSD). The parameters for ωDSD, ωDOD, and their dispersion-free variants can be found in Table S1 of the Supporting Information.

Table 1. Mean Absolute Deviations of 91 Density Functionals for Full BH9 Barrier Height Set and Its Nine Subsets[a]

Family	Functionals	ω	MAD (kcal/mol)									
			I	II	III	IV	V	VI	VII	VIII	IX	Total
B97 based	B97M-V[85]		2.41	4.77	7.50	6.18	10.18	2.75	1.38	3.59	2.82	5.18
	B97-D3BJ[86,87]		5.54	11.17	10.94	9.78	14.36	6.17	3.49	7.75	6.31	9.61
	B97[86]		4.77	11.15	6.27	4.57	5.24	6.60	3.36	2.92	5.34	6.99
	B97-1[88]		2.47	4.66	4.15	3.73	3.13	2.42	2.05	1.34	2.58	3.58
	BMK-D3BJ[87,89,90]		1.74	2.15	2.59	4.37	3.16	3.04	0.84	1.44	1.55	2.67
	BMK[89]		1.46	3.12	1.95	1.94	4.84	2.31	1.56	4.09	1.44	2.59
	ωB97X-D[91]	0.20	0.89	1.66	1.53	3.04	1.75	1.81	0.70	2.04	0.91	1.81
	ωB97X-V[20]	0.30	1.34	3.53	1.09	2.05	3.27	1.86	0.69	2.28	1.44	2.39
	ωB97M-V[21]	**0.30**	**0.70**	**1.27**	**1.21**	**1.98**	**3.09**	**1.54**	**0.55**	**1.38**	**0.84**	**1.50**
	ωB97X-2-D3BJ[87,92]	0.30	1.96	3.97	1.80	2.54	4.48	1.36	1.36	1.48	1.67	2.83
	ωB97X-2[92]	0.30	1.96	3.96	1.80	2.53	4.47	1.36	1.36	1.48	1.67	2.83
	ωB97M(2)[25]	**0.30**	**0.79**	**1.04**	**1.72**	**2.34**	**1.12**	**1.07**	**0.58**	**0.84**	**0.76**	**1.32**
PBEx-PBEc based	PBE-D3BJ[87,93,94]		5.22	10.01	12.74	12.02	16.20	6.42	6.11	7.80	6.36	10.09
	PBE[93,94]		4.52	8.00	9.80	8.50	9.87	3.80	5.48	4.35	5.17	7.41
	PBE20		1.92	3.64	4.03	4.21	4.07	2.11	3.26	1.63	2.43	3.38
	LRC-ωPBEh[12]	**0.20**	**1.55**	**2.62**	**2.33**	**2.37**	**4.51**	**2.25**	**2.31**	**4.90**	**1.11**	**2.56**
	PBE0-2-D3BJ[95,96]		3.68	3.81	2.19	2.57	6.83	2.30	1.67	1.02	1.85	3.30
	PBE0-2[95]		3.71	3.34	2.67	2.05	5.13	2.11	1.46	1.59	1.57	2.93
	SOS0-PBE0-2-D3BJ[53,97]		4.35	2.22	4.14	1.89	1.97	1.60	0.54	1.83	1.09	2.38
	SOS0-PBE0-2[97]		4.64	2.60	5.63	2.82	1.87	2.90	0.84	3.83	1.11	3.03
	PBE0-DH-D3BJ[96,98]		2.00	2.97	1.76	3.83	4.86	2.52	1.91	0.73	2.32	2.93
	PBE0-DH[98]		**1.54**	**1.95**	**1.43**	**1.90**	**1.84**	**1.34**	**1.55**	**2.88**	**1.25**	**1.77**
	SOS0-PBE0-DH-D3BJ[53,97]		1.67	2.39	1.19	2.95	3.38	2.16	1.31	1.03	1.88	2.29
	SOS0-PBE0-DH[97]		1.41	2.46	2.06	1.82	2.84	1.77	1.13	3.70	1.02	2.09
	PBE-QIDH-D3BJ[38,99]		2.06	2.89	1.29	2.32	4.63	1.79	1.49	1.15	1.82	2.46
	PBE-QIDH[38]		2.06	2.41	1.77	1.63	2.51	1.53	1.26	2.20	1.47	2.01
	SOS1-PBE-QIDH-D3BJ[99,100]		2.39	2.42	2.28	1.39	1.30	1.24	0.59	2.06	1.31	1.88
	SOS1-PBE-QIDH[100]		2.62	2.96	3.95	2.11	2.66	2.37	0.66	4.01	1.16	2.65
	RSX-QIDH-D3BJ[37,51,52]	0.27	3.37	5.40	3.62	1.34	1.57	2.47	1.76	3.71	3.11	3.34
	RSX-QIDH[37,52]	0.27	3.37	5.35	3.81	1.29	1.84	2.53	1.70	3.93	3.07	3.37
	RSX-0DH-D3BJ[51,52]	0.33	3.79	7.41	5.16	1.25	6.39	3.09	1.80	6.41	3.91	4.78
	RSX-0DH[52]	0.33	3.78	7.42	5.35	1.33	6.84	3.18	1.74	6.63	3.91	4.87
B88-LYP based	BLYP-D3BJ[87,90,101,102]		5.99	11.72	13.18	10.37	14.23	6.22	3.52	9.51	6.63	10.23
	BLYP[101,102]		5.20	11.60	8.23	5.15	5.37	6.55	3.36	3.68	5.40	7.52
	B3LYP-D3BJ[87,90,103,104]		3.09	6.11	7.08	6.04	7.71	3.79	1.58	4.53	3.70	5.54
	B3LYP[103,104]		2.94	7.47	3.69	3.11	3.74	4.98	1.57	1.91	3.65	4.67
	BH&HLYP-D3BJ[87,90,105]		1.21	3.21	2.00	1.91	4.12	2.76	2.06	2.19	1.37	2.51
	BH&HLYP[105]		1.88	6.14	5.38	5.25	11.48	5.79	3.03	5.62	2.84	5.63
	CAM-B3LYP-D3BJ[11,87,90]	**0.33**	**1.08**	**2.06**	**2.26**	**3.00**	**1.33**	**1.80**	**1.33**	**1.67**	**0.97**	**1.98**
	CAM-B3LYP[11]	0.33	1.31	3.96	2.02	2.23	6.22	3.84	1.14	3.44	1.82	3.14
	B2PLYP-D3BJ[87,106]		1.65	5.73	4.96	4.48	8.08	2.05	1.28	3.32	3.00	4.56
	B2PLYP[106]		1.57	5.01	2.83	2.29	3.67	2.52	1.18	1.40	2.34	3.21
	B2GP-PLYP-D3BJ[87,107]		1.28	4.42	2.43	2.88	6.20	1.03	0.86	1.81	2.07	3.19
	B2GP-PLYP[107]		1.40	3.56	1.30	1.67	3.03	1.87	0.74	1.00	1.59	2.29
	ωB2PLYP-D3BJ[29,51]	0.30	1.68	2.23	1.04	1.90	1.26	1.48	1.69	1.78	1.44	1.77
	ωB2PLYP[29]	0.30	1.68	2.23	1.10	1.82	1.43	1.53	1.65	1.83	1.44	1.78
	ωB2GP-PLYP-D3BJ[29,51]	0.27	2.12	1.94	1.40	1.67	1.05	1.43	1.46	1.42	1.35	1.67
	ωB2GP-PLYP[29]	**0.27**	**2.12**	**1.94**	**1.40**	**1.67**	**1.04**	**1.43**	**1.46**	**1.43**	**1.35**	**1.67**
PBE-P86 based	DSD-PBEP86-D3BJ[108]		2.28	3.70	1.65	2.97	7.27	1.47	1.27	1.66	1.98	3.14
	revDSD-PBEP86-D3BJ[109]		2.53	2.29	1.27	2.06	5.32	0.92	0.67	0.96	1.46	2.22
	revDOD-PBEP86-D3BJ[109]		2.61	1.61	1.27	1.90	4.64	0.81	0.56	0.80	1.24	1.89
	noDispSD-PBEP86[109]		2.35	4.98	1.85	3.05	7.92	1.78	1.89	1.43	2.37	3.70
	xDSD$_{75}$-PBEP86-D3BJ[36]		2.14	2.31	1.18	2.02	5.70	0.91	0.59	0.88	1.30	2.19
	xDOD$_{75}$-PBEP86-D3BJ[36]		2.29	1.30	1.15	1.82	4.81	0.76	0.45	0.68	1.00	1.73
	xnoDispSD$_{75}$-PBEP86[36]		1.99	4.42	1.84	2.90	7.95	1.56	1.46	1.33	2.03	3.41
	ωDSD$_{20}$-PBEP86-D3BJ	0.30	0.85	0.86	1.54	2.57	1.25	1.02	1.42	1.46	0.88	1.35
	ωDOD$_{20}$-PBEP86-D3BJ	**0.30**	**0.84**	**0.93**	**1.44**	**2.43**	**1.07**	**1.01**	**1.29**	**1.45**	**0.78**	**1.31**
	ωnoDispSD$_{20}$-PBEP86	0.30	1.63	4.92	4.55	5.53	6.41	2.01	4.11	2.09	2.58	4.32
	ωDSD$_{40}$-PBEP86-D3BJ	0.30	1.08	0.95	1.16	2.29	2.14	0.86	1.16	1.17	0.79	1.36
	ωDOD$_{40}$-PBEP86-D3BJ	**0.30**	**1.19**	**1.15**	**0.94**	**1.93**	**1.20**	**0.80**	**0.84**	**1.18**	**0.63**	**1.23**
	ωnoDispSD$_{40}$-PBEP86	0.30	1.24	3.71	2.93	4.10	5.73	1.71	2.96	1.61	1.88	3.29
	ωDSD$_{50}$-PBEP86-D3BJ	0.30	1.45	1.01	0.94	2.02	2.49	0.79	0.98	1.08	0.72	1.36

Table 1. continued

Family	Functionals	ω	MAD (kcal/mol)									
			I	II	III	IV	V	VI	VII	VIII	IX	Total
PBE-P86 based	ωDOD50-PBEP86-D3BJ	0.30	1.66	1.29	0.97	1.63	1.26	0.72	0.60	1.10	0.57	1.26
	ωnoDispSD50-PBEP86	0.30	1.37	3.13	1.96	3.35	5.35	1.65	2.38	1.39	1.51	2.80
	ωDSD60-PBEP86-D3BJ[36]	0.22	1.46	1.32	0.99	2.14	3.60	0.79	0.83	0.85	0.94	1.59
	ωDOD60-PBEP86-D3BJ[36]	**0.22**	**1.61**	**0.80**	**0.83**	**1.80**	**2.57**	**0.61**	**0.57**	**0.78**	**0.69**	**1.23**
	ωnoDispSD60-PBEP86[36]	0.22	1.36	4.13	2.37	3.59	6.79	1.69	2.24	1.28	1.97	3.35
	ωDSD60-PBEP86-D3BJ	0.30	2.04	1.11	1.14	1.73	2.76	0.89	0.77	1.04	0.64	1.43
	ωDOD60-PBEP86-D3BJ	0.30	2.31	1.41	1.38	1.54	1.66	0.86	0.52	1.11	0.60	1.43
	ωnoDispSD60-PBEP86	0.30	1.92	2.92	1.43	2.76	5.47	1.69	1.88	1.25	1.31	2.61
	ωDSD69-PBEP86-D3BJ[36]	0.10	1.62	1.99	1.25	2.23	5.04	0.76	0.67	0.92	1.31	2.01
	ωDOD69-PBEP86-D3BJ[36]	0.10	1.72	1.25	1.02	1.96	4.26	0.63	0.53	0.73	1.06	1.61
	ωnoDispSD69-PBEP86[36]	0.10	1.48	4.61	2.48	3.47	7.82	1.57	1.86	1.47	2.22	3.60
	ωDSD69-PBEP86-D3BJ[36]	0.16	1.83	1.83	1.06	2.09	4.64	0.86	0.70	0.74	1.10	1.89
	ωDOD69-PBEP86-D3BJ[36]	**0.16**	**1.99**	**0.85**	**0.98**	**1.73**	**3.39**	**0.65**	**0.48**	**0.61**	**0.75**	**1.36**
	ωnoDispSD69-PBEP86[36]	0.16	1.69	4.10	1.85	3.13	7.06	1.62	1.78	1.11	1.89	3.24
	ωDSD69-PBEP86-D3BJ	0.20	2.04	1.52	1.05	1.90	4.14	0.92	0.68	0.72	0.89	1.73
	ωDOD69-PBEP86-D3BJ	0.20	2.26	0.87	1.21	1.65	2.97	0.73	0.46	0.73	0.62	1.37
	ωnoDispSD69-PBEP86	0.20	1.93	3.66	1.56	2.87	6.55	1.67	1.70	1.02	1.64	2.98
	ωDSD69-PBEP86-D3BJ	0.25	2.39	1.21	1.35	1.74	3.52	1.00	0.63	0.86	0.69	1.60
	ωDOD69-PBEP86-D3BJ	0.25	2.66	1.26	1.72	1.58	2.27	0.95	0.47	1.00	0.60	1.52
	ωnoDispSD69-PBEP86	0.25	2.27	2.89	1.36	2.40	5.57	1.66	1.49	1.05	1.23	2.54
	ωDSD69-PBEP86-D3BJ	0.30	2.76	1.31	1.73	1.72	3.32	1.16	0.64	1.09	0.64	1.70
	ωDOD69-PBEP86-D3BJ	0.30	3.10	1.63	2.22	1.57	1.83	1.19	0.48	1.30	0.69	1.72
	ωnoDispSD69-PBEP86	0.30	2.67	2.54	1.52	2.19	5.18	1.71	1.35	1.19	1.02	2.41
	ωDSD72-PBEP86-D3BJ[36]	0.08	1.87	2.09	1.18	2.11	5.26	0.81	0.63	0.87	1.28	2.06
	ωDOD72-PBEP86-D3BJ[36]	0.08	1.99	1.19	1.00	1.84	4.33	0.65	0.48	0.64	0.99	1.59
	ωnoDispSD72-PBEP86[36]	0.08	1.72	4.52	2.13	3.23	7.88	1.58	1.68	1.39	2.13	3.51
	ωDSD72-PBEP86-D3BJ[36]	0.13	1.99	1.95	1.08	2.03	4.91	0.89	0.64	0.71	1.12	1.96
	ωDOD72-PBEP86-D3BJ[36]	0.13	2.17	0.93	1.08	1.74	3.80	0.71	0.45	0.57	0.80	1.46
	ωnoDispSD72-PBEP86[36]	0.13	1.86	4.12	1.77	2.97	7.24	1.61	1.61	1.12	1.89	3.23

[a]Range separation parameters (ω) are also included in a separate column. The nine reaction types of BH9 are radical rearrangement (I), Diels–Alder (II), halogen atom transfer (III), hydrogen atom transfer (IV), hydride transfer (V), boron- and silicon-containing reactions (VI), proton transfer (VII), nucleophilic substitution (VIII), and nucleophilic addition (IX).

3. RESULTS AND DISCUSSION

3.1. Barrier Heights. Table 1 gathers the performance of 91 density functional approximations on the BH9 barrier heights. In general, the range-separated hybrids clearly outperform their global counterparts for B97, PBE_x-PBE_c, and B88-LYP-based functionals.

Among the B97-family functionals, the BMK-D3BJ global hybrid outperforms the pure meta-GGA functionals B97, B97-D3BJ, and B97M-V for all nine subsets. Except for hydride transfer and nucleophilic substitution reactions, BMK is a better pick than B97−1 for the remaining subsets. With MAD = 1.50 and 1.81 kcal/mol, the range-separated hybrids, ωB97X-D and ωB97M-V, perform remarkably well. They even outperform the older range-separated double hybrid ωB97X-2 (2.83 kcal/mol), while the top performer among all B97-family functionals is Mardirossian and Head-Gordon's combinatorially optimized range-separated double hybrid ωB97M(2), with an MAD of just 1.32 kcal/mol.

Let us compare the performance of ωB97M(2) and ωB97M-V for each of the nine reaction types in BH9. For the Diels–Alder, hydride transfer, B- and Si-containing reactions, nucleophilic substitution, and nucleophilic additions, ωB97M(2) is the best pick. In contrast, for the remaining four subsets, ωB97M-V wins the race.

If we consider the PBE_x-PBE_c-based functionals, except for hydride transfer, B- and Si-containing reactions, and nucleophilic substitutions, LRC-ωPBEh outperforms its global hybrid counterpart (PBE20) for the remaining barrier heights of BH9.

Brémond et al.[76] reported the nonempirical double hybrid, PBE0-DH, as their best pick for the reduced BH9 barrier heights. Similarly, among the global double hybrid functionals of this family, PBE0-DH offers the lowest MAD (1.77 kcal/mol) when all of BH9 is considered (898 entries). Adding a D3BJ correction to any of PBE0-DH, PBE-QIDH, or PBE0-2 does more harm than good: detailed inspection of the performance statistics reveals that the dispersion corrections overstabilize the transition state relative to reactant and product, leading to systematic underestimation of barrier heights. It has already been pointed out repeatedly (see refs 48 and 84 and references therein) that if adding dispersion correction adversely affects the performance of a density functional method; it is most likely that the dispersion uncorrected form benefits from error compensation. Hence, although dispersion corrected functional does not offer better accuracy, it paints a "truer picture" of the functional suitability. Nucleophilic substitutions are the only types of reactions where all three dispersion-corrected functionals perform better than the uncorrected counterparts. That being said, for the opposite spin scaled variants of PBE0-DH and PBE-QIDH (i.e., SOS0-PBE-DH and SOS1-PBE-QIDH), dispersion-corrected forms perform better than the respective uncorrected forms. Now, going forward, similar to refs 30, 31, and 51, here too the PBE_x-PBE_c-based range-separated double hybrids are worse performers than the global double hybrids (see Table 1). Closer scrutiny of each subset reveals that range separation of the exchange term is only beneficial for the hydrogen atom transfer and hydride transfer reactions when the QIDH model is considered. On the other hand, hydrogen atom

Table 2. Mean Absolute Deviations of 91 Density Functionals for Full BH9 Reaction Energy Set and Its Nine Subsets[a]

Family	Functionals	ω	MAD (kcal/mol)									
			I	II	III	IV	V	VI	VII	VIII	IX	Total
B97 based	B97M-V[85]		1.71	5.12	3.82	2.31	2.72	1.65	1.94	1.64	2.45	3.23
	B97-D3BJ[86,87]		4.30	11.21	5.13	2.55	2.47	2.16	2.83	2.19	3.49	5.69
	B97[86]		7.18	19.98	6.19	2.87	2.19	10.74	2.83	2.63	9.80	9.92
	B97-1[88]		2.44	8.09	3.79	2.08	2.03	3.64	1.68	1.43	2.89	4.29
	BMK-D3BJ[87,89,90]		2.55	3.10	1.67	1.63	2.26	4.49	1.41	1.16	2.29	2.49
	BMK[89]		1.62	3.44	2.17	1.75	2.64	1.99	1.48	1.20	1.75	2.38
	ωB97X-D[91]	0.20	1.24	1.76	2.31	1.61	0.93	2.50	1.20	1.19	1.28	1.65
	ωB97X-V[20]	0.30	2.41	3.83	1.32	1.75	0.81	3.04	0.96	1.13	2.16	2.43
	ωB97M-V[21]	**0.30**	**1.04**	**1.46**	**1.50**	**1.21**	**1.34**	**1.98**	**0.73**	**1.11**	**1.23**	**1.36**
	ωB97X-2-D3BJ[87,92]	0.30	2.56	0.91	2.10	1.91	0.61	1.32	0.52	0.78	0.95	1.39
	ωB97X-2[92]	0.30	2.56	0.91	2.10	1.91	0.61	1.32	0.52	0.78	0.95	1.39
	ωB97M(2)[25]	**0.30**	**1.18**	**1.50**	**0.82**	**1.19**	**0.46**	**1.50**	**0.43**	**0.68**	**1.23**	**1.17**
PBEx-PBEc based	PBE-D3BJ[87,93,94]		1.89	5.35	5.63	2.91	2.81	1.39	2.87	2.74	3.61	3.73
	PBE[93,94]		2.68	8.89	6.03	3.02	2.64	4.41	2.85	2.57	2.99	5.15
	PBE20		2.05	4.76	3.85	2.10	1.49	3.02	1.84	1.61	1.91	3.07
	LRC-ωPBEh[12]	**0.20**	**2.89**	**3.21**	**2.91**	**1.88**	**1.14**	**2.41**	**1.27**	**1.19**	**1.52**	**2.42**
	PBE0-2-D3BJ[95,96]		5.45	4.79	2.76	2.75	0.60	2.77	0.66	0.65	3.51	3.40
	PBE0-2[95]		5.35	4.10	2.77	2.73	0.62	2.11	0.65	0.52	2.95	3.09
	SOS0-PBE0-2-D3BJ[53,97]		4.31	3.58	2.65	2.45	0.55	1.84	0.52	0.54	2.07	2.67
	SOS0-PBE0-2[97]		4.03	1.88	2.73	2.47	0.65	1.24	0.50	0.59	0.79	2.00
	PBE0-DH-D3BJ[96,98]		3.91	4.98	1.79	1.42	1.16	3.29	0.95	1.22	4.42	3.11
	PBE0-DH[98]		2.96	3.07	2.18	1.45	1.28	1.24	0.96	0.95	2.22	2.17
	SOS0-PBE0-DH-D3BJ[53,97]		3.26	4.13	1.76	1.34	1.19	3.15	0.91	1.21	3.59	2.70
	SOS0-PBE0-DH[97]		2.50	2.80	2.15	1.39	1.36	1.60	0.91	0.97	1.53	2.02
	PBE-QIDH-D3BJ[38,99]		3.78	4.71	1.41	1.77	0.84	2.33	0.67	0.71	3.54	2.87
	PBE-QIDH[38]		3.66	3.83	1.44	1.75	0.90	1.47	0.67	0.64	2.82	2.47
	SOS1-PBE-QIDH-D3BJ[99,100]		3.04	3.91	1.29	1.59	0.86	2.07	0.57	0.75	2.54	2.41
	SOS1-PBE-QIDH[100]		**2.77**	**2.44**	**1.42**	**1.62**	**1.00**	**1.19**	**0.56**	**0.74**	**1.18**	**1.81**
	RSX-QIDH-D3BJ[37,51,52]	0.27	6.11	10.04	1.33	1.58	1.31	3.50	0.61	1.21	6.19	5.03
	RSX-QIDH[37,52]	0.27	6.08	9.92	1.32	1.57	1.31	3.32	0.61	1.19	6.09	4.97
	RSX-0DH-D3BJ[51,52]	0.33	7.55	12.18	1.57	1.14	1.88	3.96	0.80	1.65	7.06	5.95
	RSX-0DH[52]	0.33	7.52	12.06	1.57	1.14	1.89	3.78	0.80	1.65	6.96	5.89
B88-LYP based	BLYP-D3BJ[87,90,101,102]		5.55	13.30	5.21	2.74	2.34	2.50	2.67	2.61	4.15	6.59
	BLYP[101,102]		7.85	20.68	6.08	2.96	2.34	10.28	2.67	2.54	9.76	10.19
	B3LYP-D3BJ[87,90,103,104]		3.33	8.18	3.11	1.83	2.11	1.61	1.69	1.80	2.61	4.14
	B3LYP[103,104]		5.15	14.27	3.85	2.06	2.34	7.66	1.68	1.59	7.11	7.10
	BH&HLYP-D3BJ[87,90,105]		1.69	3.37	1.74	1.55	3.39	2.39	0.80	1.88	1.37	2.37
	BH&HLYP[105]		2.89	7.79	2.24	1.77	3.73	4.92	0.81	1.88	4.35	4.37
	CAM-B3LYP-D3BJ[11,87,90]	**0.33**	**1.59**	**3.54**	**2.04**	**1.28**	**1.98**	**1.75**	**0.95**	**1.83**	**1.61**	**2.22**
	CAM-B3LYP[11]	0.33	2.36	6.72	2.41	1.42	2.24	4.50	0.93	1.47	3.56	3.70
	B2PLYP-D3BJ[87,106]		1.96	5.06	1.58	1.37	1.41	0.98	1.05	1.02	1.78	2.58
	B2PLYP[106]		2.69	7.99	1.95	1.44	1.54	3.83	1.04	1.07	3.76	3.97
	B2GP-PLYP-D3BJ[87,107]		1.87	2.95	1.39	1.58	1.33	0.83	0.65	0.80	1.24	1.87
	B2GP-PLYP[107]		2.06	5.01	1.52	1.63	1.41	2.48	0.65	0.78	2.24	2.75
	ωB2PLYP-D3BJ[29,51]	**0.30**	**2.14**	**3.33**	**1.05**	**1.08**	**1.74**	**1.98**	**0.47**	**1.28**	**2.66**	**2.11**
	ωB2PLYP[29]	**0.30**	**2.13**	**3.27**	**1.05**	**1.08**	**1.74**	**1.87**	**0.47**	**1.26**	**2.60**	**2.08**
	ωB2GP-PLYP-D3BJ[29,51]	0.27	2.64	3.23	1.32	1.38	1.62	1.80	0.49	1.08	2.62	2.18
	ωB2GP-PLYP[29]	0.27	2.64	3.23	1.32	1.38	1.62	1.79	0.49	1.08	2.62	2.18
PBE-P86 based	DSD-PBEP86-D3BJ[108]		2.94	1.09	2.07	2.10	0.62	1.51	0.68	0.83	1.59	1.58
	revDSD-PBEP86-D3BJ[109]		2.59	1.05	2.14	2.04	0.60	0.86	0.68	0.66	0.87	1.43
	revDOD-PBEP86-D3BJ[109]		2.48	0.93	2.10	2.00	0.61	0.83	0.66	0.65	0.90	1.37
	noDispSD-PBEP86[109]		3.28	1.61	2.43	2.55	0.76	1.08	0.75	0.95	1.15	1.87
	xDSD$_{75}$-PBEP86-D3BJ[36]		2.19	0.90	1.85	1.84	0.59	0.86	0.52	0.53	0.79	1.26
	xDOD$_{75}$-PBEP86-D3BJ[36]		2.09	0.70	1.85	1.80	0.59	0.82	0.55	0.52	0.77	1.17
	xnoDispSD$_{75}$-PBEP86[36]		2.65	1.32	2.08	2.28	0.79	0.97	0.58	0.74	1.02	1.60
	ωDSD$_{20}$-PBEP86-D3BJ	0.30	0.97	1.14	1.57	1.36	1.16	1.26	1.10	1.63	0.87	1.22
	ωDOD$_{20}$-PBEP86-D3BJ	0.30	0.92	1.17	1.55	1.30	1.23	1.28	1.10	1.60	0.87	1.22
	ωnoDispSD$_{20}$-PBEP86	0.30	1.85	1.90	2.25	2.17	1.82	1.46	1.42	1.83	1.58	1.91
	ωDSD$_{40}$-PBEP86-D3BJ	0.30	1.38	1.36	1.19	1.26	0.96	1.26	0.85	1.23	0.84	1.23
	ωDOD$_{40}$-PBEP86-D3BJ	0.30	1.31	1.53	1.15	1.18	1.04	1.24	0.89	1.19	0.82	1.26
	ωnoDispSD$_{40}$-PBEP86	0.30	2.12	1.69	1.64	1.89	1.33	1.24	1.02	1.31	1.35	1.65
	ωDSD$_{50}$-PBEP86-D3BJ	0.30	1.79	1.53	1.16	1.31	0.86	1.29	0.70	0.99	0.89	1.32

Table 2. continued

Family	Functionals	ω	MAD (kcal/mol)									
			I	II	III	IV	V	VI	VII	VIII	IX	Total
PBE-P86 based	ωDOD$_{50}$-PBEP86-D3BJ	0.30	1.66	1.71	1.12	1.21	0.93	1.21	0.83	0.99	0.84	1.34
	ωnoDispSD$_{50}$-PBEP86	0.30	2.46	1.66	1.52	1.92	1.11	1.24	0.81	1.05	1.28	1.64
	ωDSD$_{60}$-PBEP86-D3BJ[36]	0.22	1.67	1.06	1.23	1.33	0.70	1.07	0.68	0.79	0.77	1.13
	ωDOD$_{60}$-PBEP86-D3BJ[36]	**0.22**	**1.56**	**1.12**	**1.19**	**1.28**	**0.74**	**1.00**	**0.71**	**0.79**	**0.76**	**1.12**
	ωnoDispSD$_{60}$-PBEP86[36]	0.22	2.30	1.41	1.55	1.98	1.02	1.12	0.80	0.99	1.18	1.53
	ωDSD$_{60}$-PBEP86-D3BJ	0.30	2.35	1.82	1.54	1.55	0.74	1.35	0.56	0.79	0.98	1.55
	ωDOD$_{60}$-PBEP86-D3BJ	0.30	2.23	2.08	1.56	1.47	0.87	1.30	0.75	0.81	0.94	1.61
	ωnoDispSD$_{60}$-PBEP86	0.30	2.92	1.69	1.87	2.17	1.01	1.30	0.66	0.87	1.20	1.76
	ωDSD$_{69}$-PBEP86-D3BJ[36]	0.10	1.68	0.93	1.40	1.51	0.59	0.82	0.65	0.58	0.78	1.11
	ωDOD$_{69}$-PBEP86-D3BJ[36]	**0.10**	**1.59**	**0.78**	**1.38**	**1.48**	**0.60**	**0.80**	**0.63**	**0.56**	**0.78**	**1.04**
	ωnoDispSD$_{69}$-PBEP86[36]	0.10	2.24	1.43	1.65	2.03	0.83	0.99	0.74	0.84	1.11	1.51
	ωDSD$_{69}$-PBEP86-D3BJ[36]	0.16	1.99	0.87	1.57	1.62	0.60	0.99	0.59	0.58	0.74	1.17
	ωDOD$_{69}$-PBEP86-D3BJ[36]	0.16	1.87	0.96	1.51	1.52	0.62	0.94	0.63	0.58	0.77	1.16
	ωnoDispSD$_{69}$-PBEP86[36]	0.16	2.52	1.28	1.81	2.14	0.85	1.06	0.66	0.80	1.10	1.54
	ωDSD$_{69}$-PBEP86-D3BJ	0.20	2.25	1.13	1.69	1.69	0.62	1.12	0.52	0.60	0.79	1.32
	ωDOD$_{69}$-PBEP86-D3BJ	0.20	2.13	1.29	1.67	1.60	0.68	1.07	0.64	0.61	0.79	1.34
	ωnoDispSD$_{69}$-PBEP86	0.20	2.77	1.32	1.97	2.24	0.88	1.13	0.62	0.79	1.10	1.62
	ωDSD$_{69}$-PBEP86-D3BJ	0.25	2.62	1.63	1.86	1.80	0.65	1.30	0.49	0.61	0.94	1.58
	ωDOD$_{69}$-PBEP86-D3BJ	0.25	2.53	1.99	1.85	1.71	0.73	1.27	0.69	0.62	0.99	1.67
	ωnoDispSD$_{69}$-PBEP86	0.25	3.10	1.50	2.13	2.31	0.85	1.25	0.56	0.71	1.11	1.74
	ωDSD$_{69}$-PBEP86-D3BJ	0.30	3.06	2.08	2.10	2.01	0.69	1.46	0.52	0.61	1.08	1.85
	ωDOD$_{69}$-PBEP86-D3BJ	0.30	2.92	2.49	2.08	1.88	0.81	1.41	0.75	0.62	1.10	1.95
	ωnoDispSD$_{69}$-PBEP86	0.30	3.47	1.83	2.36	2.46	0.89	1.39	0.53	0.68	1.20	1.96
	ωDSD$_{72}$-PBEP86-D3BJ[36]	0.08	1.93	0.88	1.61	1.67	0.58	0.85	0.59	0.56	0.78	1.17
	ωDOD$_{72}$-PBEP86-D3BJ[36]	**0.08**	**1.83**	**0.71**	**1.58**	**1.61**	**0.58**	**0.82**	**0.59**	**0.53**	**0.78**	**1.09**
	ωnoDispSD$_{72}$-PBEP86[36]	0.08	2.45	1.35	1.86	2.17	0.82	0.99	0.66	0.80	1.08	1.55
	ωDSD$_{72}$-PBEP86-D3BJ[36]	0.13	2.13	0.84	1.70	1.73	0.58	0.97	0.54	0.55	0.75	1.20
	ωDOD$_{72}$-PBEP86-D3BJ[36]	0.13	2.02	0.88	1.67	1.65	0.59	0.91	0.60	0.52	0.76	1.18
	ωnoDispSD$_{72}$-PBEP86[36]	0.13	2.61	1.24	1.95	2.23	0.81	1.04	0.62	0.78	1.06	1.56

[a]Range separation parameters (ω) are included in a separate column. The nine reaction types of BH9 are radical rearrangement (I), Diels–Alder (II), halogen atom transfer (III), hydrogen atom transfer (IV), hydride transfer (V), boron- and silicon-containing reactions (VI), proton transfer (VII), nucleophilic substitution (VIII), and nucleophilic addition (IX).

transfer is the only reaction type where RSX-0DH outperforms the PBE-0DH functional.

Among the B88-LYP-based functionals, global hybrids clearly outperform the pure GGA form. Adding an empirical dispersion correction only helps hybrid functionals with a relatively large percentage of HF exchange (see Table 1). Except for the hydride transfer reactions and nucleophilic substitutions, the range-separated hybrid (i.e., CAM-B3LYP) offers better performance than B3LYP for all other barrier height subsets. However, adding dispersion on top of CAM-B3LYP noticeably improves performance for the aforementioned two subsets of BH9. With MAD = 1.98 kcal/mol, CAM-B3LYP-D3BJ even outperforms the higher-rung functionals B2PLYP and B2GP-PLYP. Unlike what we found for the PBE$_x$-PBE$_c$-based functionals, range-separated double hybrids, ωB2PLYP and ωB2GP-PLYP, offer significantly better performance than their global counterparts. Although inclusion of D3BJ degrades the performance for B2PLYP and B2GP-PLYP, it does not affect the statistics for ωB2PLYP and ωB2GP-PLYP. Except for the radical rearrangements, nucleophilic substitutions, halogen atom, and proton transfer reactions, ωB2GP-PLYP offers better performance than the corresponding global DH for the remaining five subsets. In addition to these five reaction types, ωB2PLYP outperforms the B2PLYP functional for halogen atom transfers, too.

Turning to the PBE-P86-based functionals, our revised DSD double hybrids clearly outperform the original DSD-PBEP86-D3BJ. Except for the radical rearrangement reactions, only opposite spin scaled, revDOD-PBEP86-D3BJ, performs better than the revDSD variant for the remaining eight subsets. Similar

to what we found[109] for the GMTKN55 (general main-group thermochemistry, kinetics, and noncovalent interactions, 55 problem types[48]) benchmark, xDSD$_{75}$-PBEP86-D3BJ and xDOD$_{75}$-PBEP86-D3BJ marginally outperform the corresponding revDSD and revDOD functionals, respectively. However, the revDSD-PBEP86-D3BJ functional outperforms xDSD for hydride transfer reactions. With MAD = 1.73 kcal/mol, xDOD$_{75}$-PBEP86-D3BJ is this family's best performing global double hybrid, marginally outperforming the winner of ref 76 (i.e., PBE0-DH). Like B97 and B88-LYP-family, range-separated PBE-P86-based DHs clearly outperform the global double-hybrid counterparts. With MAD = 1.23 kcal/mol, ωDOD$_{40}$-PBEP86-D3BJ (ω = 0.3) and ωDOD$_{60}$-PBEP86-D3BJ (ω = 0.22) are the two best performers for the full BH9 barrier height data set, even slightly better than ωB97M(2) (1.32 kcal/mol). Except for the proton transfer and nucleophilic substitution reactions, range separation of the exchange part benefits the performance of the seven remaining categories. Now, comparing ωDOD$_{40}$-PBEP86-D3BJ (ω = 0.3) and ωDOD$_{60}$-PBEP86-D3BJ (ω = 0.22), we found that except for the radical rearrangements, hydride transfer, and nucleophilic addition, the first one performs better than the second functional for all other subsets. For a specific value of ω (e.g., ω = 0.3), ωDOD functionals prefer a relatively small fraction of HF exchange at short-range when radical rearrangement, Diels–Alder, and hydride transfer reactions are considered. However, for the proton transfer reactions, an ωDOD functional with a large percentage of HF exchange performs better. Performance assessment of ωDOD$_{69}$-PBEP86-D3BJ functional at different
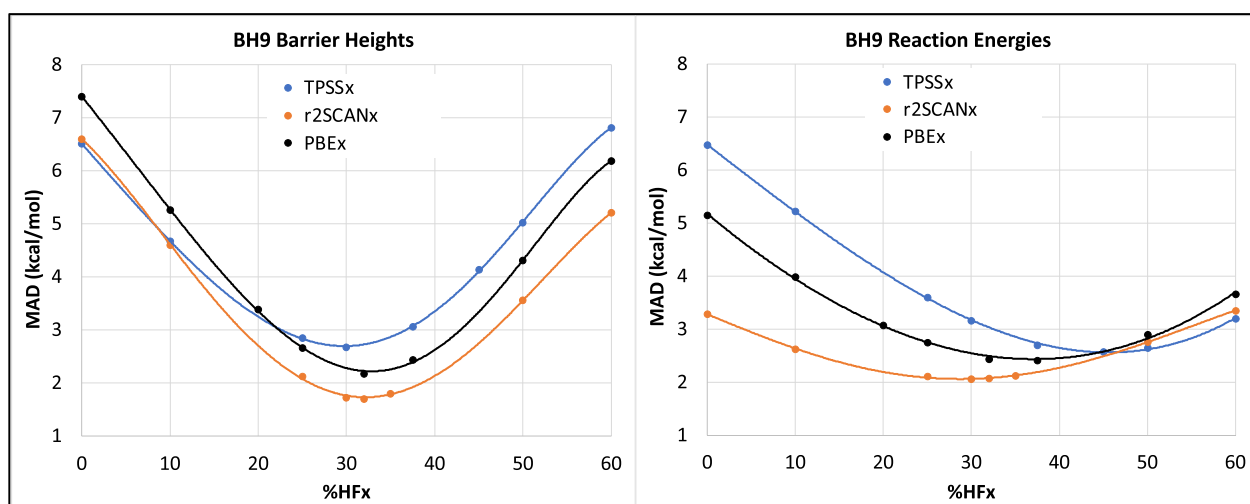
Figure 1. Dependence of mean absolute deviations (MAD, in kcal/mol) of BH9 barrier heights and reaction energies on the percentage of HF exchange for PBEx, r^{2}SCANx, and TPSSx series.

"ω" reveals that a relatively large range separation parameter is preferred for the hydrogen atom and hydride transfer reactions. In contrast, for the radical rearrangement, Diels−Alder, B- and Si-containing reactions, and nucleophilic substitutions small "ω" yields better results. Discarding the empirical dispersion correction term on average degrades performance for this family of global and range-separated double hybrid functionals.

In response to a reviewer's query, we also evaluated the performance of revPBE and PWPB95 with and without dispersion correction. For BH9 barrier heights, adding a D3BJ or D4 correction does more harm than good for both functionals. With MAD = 1.93 kcal/mol, the dispersion-uncorrected global double hybrid PWPB95 offers similar accuracy to revDOD-PBEP86-D3BJ (see Table S6 in the Supporting Information).

3.2. Reaction Energies. Table 2 gathers the mean absolute deviations of 91 dispersion-corrected and -uncorrected density functionals for the 449 reaction energies. Similar to what we found for the BH9 barrier heights, the B97, PBE$_x$-PBE$_c$, and B88-LYP-based range-separated hybrids outperform their global hybrid counterparts for BH9 reaction energies.

Among the B97-family functionals, as expected, the global hybrid performs better than the pure mGGA, and range-separated hybrids outperform the global hybrid functionals. Unlike what we found for the BH9 barrier heights, here the ωB97M-V (1.36 kcal/mol) only marginally outperforms the higher-rung functional ωB97X-2 (1.39 kcal/mol). However, with 1.17 kcal/mol mean absolute deviation, ωB97M(2) perform noticeably better than ωB97M-V. The lion's share of this improvement comes from five subsets: nucleophilic substitutions, B- and Si-containing reactions, halogen atom, hydride, and proton transfer reactions.

Turning to the PBE$_x$-PBE$_c$-based functionals, except for the radical rearrangement reactions, LRC-ωPBEh outperforms PBE20 for the remaining eight types of reaction energies. Only opposite spin-scaled PBE$_x$-PBE$_c$-based nonempirical global double hybrid functionals are more efficient than the regular DH counterparts (i.e., PBE0-2, PBE0-DH, and PBE-QIDH) for reaction energies. Similar to our observations for BH9 barrier heights, here exchange range-separation of PBE double hybrids on average impacts performance negatively. The three subsets most affected are the radical rearrangement,

Diels−Alder, and B- and Si-containing reactions. The halogen atom transfer, hydrogen atom transfer, and proton transfer reactions are the only subsets where range-separated DHs offer better accuracy than their global counterparts. SOS1-PBE-QIDH is the best performer (1.81 kcal/mol) among all the functionals tested of this family.

Next, among the B88-LYP-based functionals, range-separated hybrid outperforms the global hybrids functionals when the full BH9 reaction energy set is considered. Adding an empirical dispersion correction helps improve the performance of both global and range-separated hybrids. CAM-B3LYP-D3BJ outperforms the B3LYP-D3BJ for all reaction energies except B- and Si-containing reactions. The D3BJ-corrected B88-LYP-based global double hybrids (i.e., B2PLYP-D3BJ and B2GP-PLYP-D3BJ) offer lower MAD values than their uncorrected counterparts. Interestingly enough, range separation of the exchange part only helps for B2PLYP-D3BJ, but for the B2GP-PLYP-D3BJ, it does the opposite (see Table 2). Three subsets where ωB2PLYP-D3BJ and ωB2GP-PLYP-D3BJ offer better performance than their global DH counterparts are halogen atom, hydrogen atom, and proton transfer reactions. With 1.87 kcal/mol mean absolute deviation, B2GP-PLYP-D3BJ is the best pick among all the B88-LYP family functionals tested in the present study.

Now, if we consider the PBE-P86-based global and range-separated DHs, revDSD-PBEP86-D3BJ clearly outperforms the original DSD-PBEP86-D3BJ functional. Similar to BH9 barrier heights, here, revDOD-PBEP86-D3BJ and xDOD$_{75}$-PBEP86-D3BJ offer better accuracy than their DSD counterparts. A significant share of this performance improvement comes from the radical rearrangement and Diels−Alder reactions. If all 449 reaction energies are considered, xDOD$_{75}$-PBEP86-D3BJ performs similarly to the range-separated Berkeley double hybrid ωB97M(2) (see Table 2). Comparing these two functionals for nine subsets, we found that except for Diels−Alder, B- and Si-containing reactions, nucleophilic substitution, and addition reactions, ωB97M(2) outperforms global double hybrid xDOD$_{75}$-PBEP86-D3BJ for all other subsets. A number of our range-separated ωDSD functionals offer better accuracy than the best global double hybrid of this family, xDOD$_{75}$-PBEP86-D3BJ. Hence, range separation of the exchange part of our DSD-family double hybrids clearly benefits for the BH9

Table 3. Mean Absolute Deviations of Different Pure and Hybrid GGA and Meta-GGA Functionals for Full BH9 Barrier Height Set and Its Nine Subsets[a]

Functionals	MAD (kcal/mol)									
	I	II	III	IV	V	VI	VII	VIII	IX	Total
PBE[93,94]	4.52	8.00	9.80	8.50	9.87	3.80	5.48	4.35	5.17	7.41
PBE10	3.08	5.69	6.69	6.24	6.99	2.85	4.36	2.26	3.80	5.26
PBE20	1.92	3.64	4.03	4.21	4.07	2.11	3.26	1.63	2.43	3.38
PBE0[110,111]	1.56	2.85	2.89	3.35	2.99	1.86	2.72	1.98	1.81	2.66
PBE32	1.39	2.30	1.95	2.51	2.82	1.73	2.01	3.23	1.27	2.18
PBE38[90]	1.52	2.74	2.23	2.19	3.92	1.95	1.46	4.27	1.23	2.44
PBE50	2.24	5.39	5.12	2.88	7.69	2.95	1.13	6.54	2.28	4.31
PBE60	2.87	7.89	7.69	4.30	10.92	3.78	1.41	8.18	3.51	6.19
r²SCAN[112,113]	3.32	7.14	8.37	7.50	10.68	2.80	3.87	4.64	4.53	6.61
r²SCANh[114]	2.36	4.93	5.67	5.38	7.46	1.97	2.96	2.57	3.32	4.61
r²SCAN0[114]	1.35	2.32	2.20	2.59	2.79	1.19	1.77	1.19	1.61	2.12
r²SCAN30	1.26	1.92	1.55	2.01	2.01	1.16	1.53	1.79	1.34	1.73
r²SCAN32	1.25	1.91	1.48	1.87	2.04	1.21	1.48	2.09	1.29	1.71
r²SCAN35	1.27	2.05	1.68	1.74	2.43	1.34	1.41	2.58	1.23	1.81
r²SCAN50[114]	1.80	4.33	4.37	2.63	6.34	2.26	1.14	5.07	1.95	3.57
r²SCAN60	2.26	6.53	6.45	3.94	9.43	2.86	1.38	6.62	2.90	5.21
TPSS[115]	4.44	8.83	7.81	5.55	6.08	4.55	3.81	4.31	4.71	6.51
TPSSh[116]	3.16	6.59	5.01	4.01	3.86	3.83	2.81	2.46	3.39	4.68
TPSS0[117]	1.62	3.67	2.32	2.70	3.65	2.91	1.46	2.33	1.67	2.86
TPSS30	1.30	3.05	2.23	2.63	4.67	2.75	1.14	2.93	1.25	2.68
TPSS38	1.26	3.04	3.33	2.97	6.60	2.77	1.02	4.19	1.20	3.06
TPSS45	1.58	4.37	4.97	3.71	8.72	3.26	1.30	5.52	1.84	4.14
TPSS50	1.91	5.59	6.22	4.30	10.14	3.60	1.65	6.42	2.45	5.03
TPSS60	2.59	8.11	8.58	5.52	12.97	4.27	2.40	8.12	3.68	6.82
PBE-D3BJ[87,93,94]	5.22	10.01	12.74	12.02	16.20	6.42	6.11	7.80	6.36	10.09
PBE0-D3BJ[87,110,111]	2.10	3.73	4.97	6.21	7.88	3.27	3.10	1.75	2.87	4.40
PBE38-D3BJ[87,90]	1.82	2.51	1.54	3.50	3.44	2.20	1.76	1.28	2.10	2.52
r²SCAN-D3BJ[114]	3.59	8.05	9.85	9.17	14.09	4.32	4.31	6.34	5.04	7.93
r²SCANh-D3BJ[114]	2.65	5.85	7.22	7.11	11.04	3.41	3.38	4.22	3.85	5.96
r²SCAN0-D3BJ[114]	1.62	3.04	3.38	4.23	6.28	2.38	2.13	1.40	2.20	3.29
r²SCAN50-D3BJ[114]	1.91	3.61	2.83	1.64	2.81	2.44	1.38	3.06	2.05	2.64
TPSS-D3BJ[90,115]	5.26	10.59	11.50	9.54	13.30	6.14	4.13	8.74	6.08	9.33
TPSSh-D3BJ[90,116]	3.90	7.82	8.48	7.44	10.34	4.93	3.05	6.21	4.65	7.06
TPSS0-D3BJ[90,117]	2.30	4.14	4.05	4.49	5.41	3.22	1.60	2.77	2.60	3.86

[a]Nine subsets of BH9 are radical rearrangement (I), Diels−Alder (II), halogen atom transfer (III), hydrogen atom transfer (IV), hydride transfer (V), boron- and silicon-containing reactions (VI), proton transfer (VII), nucleophilic substitution (VIII), and nucleophilic addition (IX).

reaction energies. Unlike for BH9 barrier heights, the overall performance of the ωDSD and ωDOD-PBEP86-D3BJ functionals are comparable for reactions energies. With 1.04 kcal/mol mean absolute deviation, the ωDOD$_{69}$-PBEP86-D3BJ (ω = 0.10) is the best pick among the PBE-P86 family as well as all the functionals tested in the present study for BH9 reactions energies. Comparing the performance of best global and range-separated DHs of this family, we found that radical rearrangements, halogen, and hydrogen atom transfer reactions enjoy the lion's share of the benefit from range separation.

Opposite of what we found for BH9 barrier heights, for reaction energies, adding a dispersion correction significantly improves the accuracy of revPBE and PWPB95 (see Table S7 in the Supporting Information). Our revDSD- and revDOD-PBEP86-D3BJ marginally outperformed PWPB95-D3BJ.

Now, what if we gradually increase the percentage of short-range HF exchange while keeping the range separation parameter (ω) fixed? Except for hydride transfer, proton transfer, and nucleophilic substitution reactions, ωDSD func-

tionals prefer 50% or less short-range HF exchange for all other reactions. We have also checked the performance of ωDSD$_{69}$-PBEP86-D3BJ at five different values of ω ranging from 0.1 to 0.3. Interestingly, for the hydride transfer, proton transfer, and nucleophilic substitution reactions, the range separation parameter has little to no influence on the mean absolute deviations.

Next, to answer the second research question, we have considered pure and hybrid PBE,[93,94] TPSS,[115] and r²SCAN,[112,113] varying the percentage of exact exchange from 10 to 60% for hybrid GGA and meta-GGA functionals. Considering the 898 barrier heights of BH9, we obtained the best performance near 33% (∼1/3) HF exchange for the PBEx and r²SCANx series (where x represents the percentage of exact exchange used in the hybrid functional). However, among the TPSS-based hybrids, TPSS30 offers marginally lower MAD than TPSS33 (see Figure 1, left). For BH9 reaction energies, we obtain the best performance near 38%, 45%, and 30% HF

Table 4. Mean Absolute Deviations of Different Pure and Hybrid GGA and Meta-GGA Functionals for Full BH9 Reaction Energy Set and Its Nine Subsets[a]

Functionals	MAD (kcal/mol)									
	I	II	III	IV	V	VI	VII	VIII	IX	Total
PBE[93,94]	2.68	8.89	6.03	3.02	2.64	4.41	2.85	2.57	2.99	5.15
PBE10	2.15	6.67	4.84	2.51	1.76	3.72	2.33	2.09	2.39	3.99
PBE20	2.05	4.76	3.85	2.10	1.49	3.02	1.84	1.61	1.91	3.07
PBE0[110,111]	2.16	4.04	3.52	1.95	1.47	2.70	1.63	1.44	1.75	2.75
PBE32	2.47	3.35	3.07	1.73	1.53	2.25	1.31	1.23	1.74	2.44
PBE38[90]	2.80	3.33	2.79	1.60	1.75	2.02	1.10	1.22	1.86	2.42
PBE50	3.86	4.50	2.34	1.47	2.37	1.68	0.77	1.43	2.54	2.90
PBE60	4.82	6.18	2.18	1.57	2.87	2.05	0.94	1.84	3.34	3.67
r^{2}SCAN[112,113]	1.39	5.64	4.36	2.07	1.71	1.67	2.21	1.69	2.58	3.28
r^{2}SCANh[114]	1.33	4.21	3.57	1.75	1.59	1.47	1.81	1.50	2.23	2.63
r^{2}SCAN0[114]	1.77	2.85	2.80	1.42	1.88	1.46	1.25	1.35	2.03	2.11
r^{2}SCAN30	2.02	2.64	2.63	1.35	2.06	1.54	1.10	1.32	2.03	2.06
r^{2}SCAN32	2.13	2.64	2.57	1.33	2.14	1.57	1.04	1.32	2.05	2.07
r^{2}SCAN35	2.30	2.73	2.49	1.32	2.26	1.64	0.95	1.35	2.09	2.12
r^{2}SCAN50[114]	3.29	4.02	2.16	1.47	2.85	2.23	0.81	1.56	2.52	2.76
r^{2}SCAN60	3.98	5.14	2.15	1.73	3.22	2.70	0.89	1.89	3.06	3.35
TPSS[115]	3.45	12.19	5.66	2.97	2.66	6.81	2.32	2.42	4.41	6.47
TPSSh[116]	2.68	9.68	4.61	2.58	1.82	5.92	1.88	2.08	3.64	5.22
TPSS0[117]	1.95	6.16	3.47	2.21	1.31	4.54	1.28	1.77	2.34	3.60
TPSS30	1.97	5.10	3.17	2.14	1.31	4.06	1.08	1.73	1.92	3.17
TPSS38	2.21	3.91	2.83	2.06	1.51	3.40	0.90	1.69	1.42	2.71
TPSS45	2.63	3.54	2.55	2.03	1.84	2.83	0.88	1.71	1.15	2.57
TPSS50	3.02	3.67	2.39	2.03	2.10	2.53	0.94	1.79	1.19	2.65
TPSS60	3.99	4.78	2.33	2.13	2.67	2.29	1.08	2.08	1.97	3.20
PBE-D3BJ[87,93,94]	1.89	5.35	5.63	2.91	2.81	1.39	2.87	2.74	3.61	3.73
PBE0-D3BJ[87,110,111]	2.43	2.35	3.10	1.84	1.25	2.20	1.65	1.46	3.44	2.23
PBE38-D3BJ[87,90]	3.52	4.12	2.40	1.54	1.56	3.03	1.10	1.45	3.98	2.88
r^{2}SCAN-D3BJ[114]	1.27	4.38	4.23	2.03	1.71	2.01	2.23	1.81	3.16	2.92
r^{2}SCANh-D3BJ[114]	1.33	3.02	3.42	1.71	1.51	2.21	1.83	1.65	2.95	2.33
r^{2}SCAN0-D3BJ[114]	2.04	2.26	2.64	1.39	1.79	2.78	1.27	1.48	2.88	2.08
r^{2}SCAN50-D3BJ[114]	3.72	5.08	1.98	1.47	2.70	4.00	0.82	1.60	3.82	3.32
TPSS-D3BJ[90,115]	2.19	7.44	5.11	2.87	2.90	2.14	2.34	2.11	2.69	4.34
TPSSh-D3BJ[90,116]	1.60	5.17	4.08	2.50	1.98	2.03	1.90	1.85	2.26	3.26
TPSS0-D3BJ[90,117]	1.78	2.02	2.90	2.15	1.17	2.31	1.29	1.61	2.24	2.03

[a]Nine subsets of BH9 are radical rearrangement (I), Diels−Alder (II), halogen atom transfer (III), hydrogen atom transfer (IV), hydride transfer (V), boron- and silicon-containing reactions (VI), proton transfer (VII), nucleophilic substitution (VIII), and nucleophilic addition (IX).

exchange for the PBE, TPSS, and r^{2}SCAN-based functionals, respectively (see Figure 1, right).

Irrespective of GGA or mGGA functional choice, using a small fraction of HF exchange underestimates the barrier heights, while a higher fraction overestimates them. On the other hand, the trend is the opposite for the reaction energies (see Tables S4 and S5 in the Supporting Information).

For BH9 barrier heights, adding a D3BJ dispersion correction does more harm than good for pure and hybrid functionals with 25% or less HF exchange. This behavior again hints at problems with the suitability of the functional itself. However, for the reaction energies, dispersion corrected forms of these functionals offer better accuracy than the uncorrected ones (see Tables 3 and 4).

Closer scrutiny of the performance of nine different reaction energy subsets reveals that for the Diels−Alder reactions, PBE, TPSS, and r^{2}SCAN-based hybrids perform best near 38%, 45%, and 33% HF exchange, respectively. However, for the nucleophilic substitutions, both the PBEx and TPSSx series

have minima near the same percentage (38%), whereas the r^{2}SCANx series offers the lowest MAD near 33%. A comparatively lower percentage (∼20−25%) of HF exchange is preferred by PBEx and r^{2}SCANx series for the radical rearrangements and hydride transfer reactions. For the halogen atom transfer, B- and Si-containing reactions, hydrogen atom, and proton transfer reactions, the PBE and TPSS-based hybrids with a relatively large percentage of exact exchanges offer the best accuracy. However, among the r^{2}SCAN-based hybrids, the first two types of reactions prefer a fairly large, and the last two a fairly small, percentage of HF exchange. Finally, the best performers for the nucleophilic addition reactions are PBE32, r^{2}SCAN30, and TPSS45 (see Table 4).

Thus far, we have considered the older D3BJ and nonlocal VV10 dispersion corrections. A reviewer inquired what happens if we use D4 instead, which includes both partial charge dependence and three-body corrections? A small test using ten selected functionals suggests that for BH9 barrier heights, range-separated hybrid and double hybrids do not benefit from

Table 5. Mean Absolute Deviations of Pure and Hybrid Self-Consistent and HF-DFT Functionals for BH9 Barrier Heights and Reaction Energies[a]

Functionals	MAD (kcal/mol)									
	Barrier Heights									
	I	II	III	IV	V	VI	VII	VIII	IX	Total
PBE[93,94]	4.52	8.00	9.80	8.50	9.87	3.80	5.48	4.35	5.17	7.41
HF-PBE[118]	4.43	7.93	8.25	6.69	7.62	4.75	3.42	5.53	3.52	6.62
PBE0[110,111]	1.56	2.85	2.89	3.35	2.99	1.86	2.72	1.98	1.81	2.66
HF-PBE0[119]	4.44	3.09	9.64	6.27	2.98	4.26	1.59	6.85	1.35	4.57
PBE-D4[93,94,120]	5.29	10.17	12.95	12.18	16.20	6.64	6.24	8.03	6.50	10.23
HF-PBE-D4[119]	3.57	9.92	6.02	5.80	14.54	3.28	3.91	2.13	4.69	7.26
PBE0[110,111,120]	2.16	3.84	5.05	6.27	7.75	3.33	3.20	1.87	2.96	4.46
HF-PBE0-D4[119]	3.88	4.02	6.60	4.00	6.14	2.07	1.93	2.88	2.14	4.10
Functionals	Reaction Energies									
PBE[93,94]	2.68	8.89	6.03	3.02	2.64	4.41	2.85	2.57	2.99	5.15
HF-PBE[118]	3.77	8.46	7.14	6.90	1.37	8.16	1.75	2.49	4.21	6.24
PBE0[110,111]	2.16	4.04	3.52	1.95	1.47	2.70	1.63	1.44	1.75	2.75
HF-PBE0[119]	4.05	4.08	5.11	4.74	1.26	4.79	1.24	1.55	1.70	3.82
PBE-D4[93,94,120]	1.86	4.93	5.65	2.92	2.63	1.35	2.81	2.84	3.71	3.59
HF-PBE-D4[119]	3.72	3.40	6.99	6.90	1.26	3.25	1.69	2.05	2.06	4.11
PBE0[110,111,120]	2.59	2.49	3.14	1.85	1.33	2.13	1.60	1.50	3.61	2.31
HF-PBE0-D4[119]	4.75	3.19	4.97	4.73	1.16	2.84	1.20	1.19	2.78	3.48

[a]Nine subsets of BH9 are radical rearrangement (I), Diels−Alder (II), halogen atom transfer (III), hydrogen atom transfer (IV), hydride transfer (V), boron- and silicon-containing reactions (VI), proton transfer (VII), nucleophilic substitution (VIII), and nucleophilic addition (IX).

substituting D4 for D3BJ (see Table S6 in the Supporting Information). However, global double hybrid functionals, xDSD-PBEP86-D4 and xDOD-PBEP86-D4 perform marginally better than their D3BJ corrected counterparts. For barrier heights, D4 on average somewhat spoils performance for PBE, but B97-D4 performs significantly better than B97-D3BJ. Now, for the BH9 reaction energies, ωB97X-D3BJ performs better than ωB97X-D4. However, using D4 dispersion correction instead of D3BJ has no additional benefit for our DSD-family range separated and global double hybrids. For reaction energies, B97-D3BJ offers better accuracy than B97-D4 (see Table S7 in the Supporting Information).

In previous studies, Sim and Burke,[121,122] the Goerigk group,[84] and the present authors[119,123] have shown that the use of HF densities instead of self-consistent KS densities can significantly improve the performance of pure and hybrid (with 25% or less exact exchange) GGA and mGGA functionals for noncovalent interactions and barrier heights. Except for the B- and Si-containing reactions and nucleophilic substitutions, HF-PBE outperforms its self-consistent counterpart, PBE, for the remaining seven subsets of BH9 barrier heights. However, with a D4 dispersion correction, HF-PBE-D4 fares better than PBE-D4 throughout. Using the HF density on average is detrimental for PBE0, but with D4 dispersion correction, HF-PBE0-D4 marginally outperforms PBE0-D4 (see Table 5).

Now, for the BH9 reaction energies, self-consistent functionals perform better than the density-corrected counterparts except for hydride and proton transfer reactions. Using the D4 dispersion correction only reduces the mean absolute error of each functional without affecting the trend (see Table 5).

IV. CONCLUSIONS

From an extensive survey of global and range-separated hybrid and double hybrid functionals using a large and, more importantly, diverse data set for barrier heights and reaction energies, we can conclude the following:

- Both for the BH9 barrier heights and reaction energies, B97, PBE_x-PBE_c, and B88-LYP-family range-separated hybrids functionals outperform their global hybrid counterparts.

- Except for the PBE_x-PBE_c-family functionals, the range-separated double hybrid functionals perform significantly better than the corresponding global double hybrids for BHs and REs.

- RSX-PBE-QIDH and RSX-PBE-0DH offer better accuracy than the respective global counterparts only for the barrier heights of hydrogen atom transfer reactions. However, among the nine subsets of the BH9 reaction energies, halogen atom transfer, hydrogen atom transfer, and proton transfer reactions are the only three subsets that benefit from range separation in the same family.

- Among all the functionals tested here, ωDOD$_{40}$-PBEP86-D3BJ ($\omega = 0.3$) and ωDOD$_{60}$-PBEP86-D3BJ ($\omega = 0.22$) are the two best picks (MAD = 1.23 kcal/mol) for barrier heights and ωDOD$_{69}$-PBEP86-D3BJ ($\omega = 0.10$) is the best pick for reaction energies overall. Using the more modern D4 dispersion correction instead of D3BJ imparts no additional benefit. In previous work[36] for the GMTKN55 benchmark, we found that our six-parameter empirical range-separated double hybrids slightly outperform Mardirossian and Head-Gordon's 16-parameter range-separated double hybrid ωB97M(2); for the BH9 set considered here, we find a somewhat more pronounced advantage.

- PBE and r²SCAN-based hybrid functionals offer the lowest mean absolute deviation for BH9 barrier heights near 33% (~1/3) HF exchange, whereas for the TPSSx series, it is near 30%. However, for the reaction energies, we obtain the best performance near 38%, 45%, and 30% for the PBEx, TPSSx, and r²SCANx series, respectively.

■ ASSOCIATED CONTENT

ⓢ Supporting Information

The Supporting Information is available free of charge at https://pubs.acs.org/doi/10.1021/acs.jpca.2c03922.

Optimized parameters for our ωDSD-PBEP86-D3BJ, ωDOD-PBEP86-D3BJ, and ωnoDispSD-PBEP86 functionals; RMSD for different DFT functionals; MSD for different DFT functionals; MAD for some additional functionals (PDF)

■ AUTHOR INFORMATION

Corresponding Author

Jan M. L. Martin − *Department of Molecular Chemistry and Materials Science, Weizmann Institute of Science, 7610001 Reḥovot, Israel;* ⓞ orcid.org/0000-0002-0005-5074; Email: gershom@weizmann.ac.il

Authors

Golokesh Santra − *Department of Molecular Chemistry and Materials Science, Weizmann Institute of Science, 7610001 Reḥovot, Israel;* ⓞ orcid.org/0000-0002-7297-8767

Rivka Calinsky − *Department of Molecular Chemistry and Materials Science, Weizmann Institute of Science, 7610001 Reḥovot, Israel*

Complete contact information is available at:
https://pubs.acs.org/10.1021/acs.jpca.2c03922

■ REFERENCES

(1) Bachrach, S. M. Challenges in Computational Organic Chemistry. *WIREs Comput. Mol. Sci.* **2014**, *4* (5), 482−487.

(2) Houk, K. N.; Liu, F. Holy Grails for Computational Organic Chemistry and Biochemistry. *Acc. Chem. Res.* **2017**, *50* (3), 539−543.

(3) Curtiss, L. A.; Redfern, P. C.; Raghavachari, K. G*n* Theory. *WIREs Comput. Mol. Sci.* **2011**, *1* (5), 810−825.

(4) Karton, A. A Computational Chemist's Guide to Accurate Thermochemistry for Organic Molecules. *Wiley Interdiscip. Rev. Comput. Mol. Sci.* **2016**, *6* (3), 292−310.

(5) Martin, J. M. L. Chapter 3 Computational Thermochemistry: A Brief Overview of Quantum Mechanical Approaches. *Annu. Rep. Comput. Chem.* **2005**, *1* (05), 31−43.

(6) Helgaker, T.; Klopper, W.; Tew, D. P. Quantitative Quantum Chemistry. *Mol. Phys.* **2008**, *106* (16−18), 2107−2143.

(7) Peterson, K. A.; Feller, D.; Dixon, D. A. Chemical Accuracy in Ab Initio Thermochemistry and Spectroscopy: Current Strategies and Future Challenges. *Theor. Chem. Acc.* **2012**, *131* (1), 1079.

(8) Chan, B. How to Computationally Calculate Thermochemical Properties Objectively, Accurately, and as Economically as Possible. *Pure Appl. Chem.* **2017**, *89* (6), 699−713.

(9) Kohn, W.; Sham, L. J. Self-Consistent Equations Including Exchange and Correlation Effects. *Phys. Rev.* **1965**, *140* (4A), A1133−A1138.

(10) Perdew, J. P.; Schmidt, K. Jacob's Ladder of Density Functional Approximations for the Exchange-Correlation Energy. *AIP Conf. Proc.* **2001**, *577* (1), 1−20.

(11) Yanai, T.; Tew, D. P.; Handy, N. C. A New Hybrid Exchange−Correlation Functional Using the Coulomb-Attenuating Method (CAM-B3LYP). *Chem. Phys. Lett.* **2004**, *393* (1−3), 51−57.

(12) Rohrdanz, M. A.; Martins, K. M.; Herbert, J. M. A Long-Range-Corrected Density Functional That Performs Well for Both Ground-State Properties and Time-Dependent Density Functional Theory Excitation Energies, Including Charge-Transfer Excited States. *J. Chem. Phys.* **2009**, *130* (5), No. 054112.

(13) Henderson, T. M.; Izmaylov, A. F.; Scalmani, G.; Scuseria, G. E. Can Short-Range Hybrids Describe Long-Range-Dependent Properties? *J. Chem. Phys.* **2009**, *131* (4), No. 044108.

(14) Iikura, H.; Tsuneda, T.; Yanai, T.; Hirao, K. A Long-Range Correction Scheme for Generalized-Gradient-Approximation Exchange Functionals. *J. Chem. Phys.* **2001**, *115* (8), 3540−3544.

(15) Peverati, R.; Truhlar, D. G. Improving the Accuracy of Hybrid Meta-GGA Density Functionals by Range Separation. *J. Phys. Chem. Lett.* **2011**, *2* (21), 2810−2817.

(16) Chai, J.-D.; Head-Gordon, M. Systematic Optimization of Long-Range Corrected Hybrid Density Functionals. *J. Chem. Phys.* **2008**, *128* (8), No. 084106.

(17) Manna, A. K.; Refaely-Abramson, S.; Reilly, A. M.; Tkatchenko, A.; Neaton, J. B.; Kronik, L. Quantitative Prediction of Optical Absorption in Molecular Solids from an Optimally Tuned Screened Range-Separated Hybrid Functional. *J. Chem. Theory Comput.* **2018**, *14* (6), 2919−2929.

(18) Baer, R.; Livshits, E.; Salzner, U. Tuned Range-Separated Hybrids in Density Functional Theory. *Annu. Rev. Phys. Chem.* **2010**, *61* (1), 85−109.

(19) Vydrov, O. A.; Heyd, J.; Krukau, A. V.; Scuseria, G. E. Importance of Short-Range versus Long-Range Hartree-Fock Exchange for the Performance of Hybrid Density Functionals. *J. Chem. Phys.* **2006**, *125* (7), No. 074106.

(20) Mardirossian, N.; Head-Gordon, M. ωB97X-V: A 10-Parameter, Range-Separated Hybrid, Generalized Gradient Approximation Density Functional with Nonlocal Correlation, Designed by a Survival-of-the-Fittest Strategy. *Phys. Chem. Chem. Phys.* **2014**, *16* (21), 9904.

(21) Mardirossian, N.; Head-Gordon, M. ωB97M-V: A Combinatorially Optimized, Range-Separated Hybrid, Meta-GGA Density Functional with VV10 Nonlocal Correlation. *J. Chem. Phys.* **2016**, *144* (21), 214110.

(22) Ángyán, J. G.; Gerber, I. C.; Savin, A.; Toulouse, J. van der Waals Forces in Density Functional Theory: Perturbational Long-Range Electron-Interaction Corrections. *Phys. Rev. A* **2005**, *72* (1), No. 012510.

(23) Benighaus, T.; Distasio, R. A.; Lochan, J. R. C.; Chai, J. Da; Head-Gordon, M. Semiempirical Double-Hybrid Density Functional with Improved Description of Long-Range Correlation. *J. Phys. Chem. A* **2008**, *112* (12), 2702−2712.

(24) Görling, A.; Levy, M. Exact Kohn-Sham Scheme Based on Perturbation Theory. *Phys. Rev. A* **1994**, *50* (1), 196−204.

(25) Mardirossian, N.; Head-Gordon, M. Survival of the Most Transferable at the Top of Jacob's Ladder: Defining and Testing the ωB97M(2) Double Hybrid Density Functional. *J. Chem. Phys.* **2018**, *148* (24), 241736.

(26) Zhang, Y.; Xu, X.; Goddard, W. A. Doubly Hybrid Density Functional for Accurate Descriptions of Nonbond Interactions, Thermochemistry, and Thermochemical Kinetics. *Proc. Natl. Acad. Sci. U. S. A.* **2009**, *106* (13), 4963−4968.

(27) Kesharwani, M. K.; Kozuch, S.; Martin, J. M. L. Comment on "Doubly Hybrid Density Functional xDH-PBE0 from a Parameter-Free Global Hybrid Model PBE0" [J. Chem. Phys. 136, 174103 (2012)]. *J. Chem. Phys.* **2015**, *143* (18), 187101.

(28) Santra, G.; Martin, J. M. L. Does GLPT2 Offer Any Actual Benefit Over Conventional HF-MP2 In the Context of Double-Hybrid Density Functionals? *AIP Conf. Proc.* **2022**. http://arxiv.org/abs/2111.01880.

(29) Casanova-Páez, M.; Dardis, M. B.; Goerigk, L. ωB2PLYP and ωB2GPPLYP: The First Two Double-Hybrid Density Functionals with Long-Range Correction Optimized for Excitation Energies. *J. Chem. Theory Comput.* **2019**, *15* (9), 4735−4744.

(30) Casanova-Páez, M.; Goerigk, L. Time-Dependent Long-Range-Corrected Double-Hybrid Density Functionals with Spin-Component and Spin-Opposite Scaling: A Comprehensive Analysis of Singlet−Singlet and Singlet−Triplet Excitation Energies. *J. Chem. Theory Comput.* **2021**, *17* (8), 5165−5186.

(31) Casanova-Páez, M.; Goerigk, L. Assessing the Tamm−Dancoff Approximation, Singlet−Singlet, and Singlet−Triplet Excitations with the Latest Long-Range Corrected Double-Hybrid Density Functionals. *J. Chem. Phys.* **2020**, *153* (6), No. 064106.

(32) Mester, D.; Kállay, M. Combined Density Functional and Algebraic-Diagrammatic Construction Approach for Accurate Excitation Energies and Transition Moments. *J. Chem. Theory Comput.* **2019**, *15* (8), 4440−4453.

(33) Mester, D.; Kállay, M. A Simple Range-Separated Double-Hybrid Density Functional Theory for Excited States. *J. Chem. Theory Comput.* **2021**, *17* (2), 927−942.

(34) Mester, D.; Kállay, M. Spin-Scaled Range-Separated Double-Hybrid Density Functional Theory for Excited States. *J. Chem. Theory Comput.* **2021**, *17* (7), 4211−4224.

(35) Mester, D.; Kállay, M. Accurate Spectral Properties within Double-Hybrid Density Functional Theory: A Spin-Scaled Range-Separated Second-Order Algebraic-Diagrammatic Construction-Based Approach. *J. Chem. Theory Comput.* **2022**, *18* (2), 865−882.

(36) Santra, G.; Cho, M.; Martin, J. M. L. Exploring Avenues beyond Revised DSD Functionals: I. Range Separation, with x DSD as a Special Case. *J. Phys. Chem. A* **2021**, *125* (21), 4614−4627.

(37) Brémond, É.; Savarese, M.; Pérez-Jiménez, Á. J.; Sancho-García, J. C.; Adamo, C. Range-Separated Double-Hybrid Functional from Nonempirical Constraints. *J. Chem. Theory Comput.* **2018**, *14* (8), 4052−4062.

(38) Brémond, É.; Sancho-García, J. C.; Pérez-Jiménez, Á. J.; Adamo, C. Communication: Double-Hybrid Functionals from Adiabatic-Connection: The QIDH Model. *J. Chem. Phys.* **2014**, *141* (3), No. 031101.

(39) Toulouse, J.; Colonna, F.; Savin, A. Long-Range−Short-Range Separation of the Electron-Electron Interaction in Density-Functional Theory. *Phys. Rev. A* **2004**, *70* (6), No. 062505.

(40) Kalai, C.; Toulouse, J. A General Range-Separated Double-Hybrid Density-Functional Theory. *J. Chem. Phys.* **2018**, *148* (16), 164105.

(41) Prokopiou, G.; Hartstein, M.; Govind, N.; Kronik, L. Optimal Tuning Perspective of Range-Separated Double Hybrid Functionals. *J. Chem. Theory Comput.* **2022**, *18* (4), 2331−2340.

(42) Assfeld, X.; Almlöf, J. E.; Truhlar, D. G. Degeneracy-Corrected Perturbation Theory for Electronic Structure Calculations. *Chem. Phys. Lett.* **1995**, *241* (4), 438−444.

(43) Neese, F.; Schwabe, T.; Grimme, S. Analytic Derivatives for Perturbatively Corrected "Double Hybrid" Density Functionals: Theory, Implementation, and Applications. *J. Chem. Phys.* **2007**, *126* (12), 124115.

(44) Biczysko, M.; Panek, P.; Scalmani, G.; Bloino, J.; Barone, V. Harmonic and Anharmonic Vibrational Frequency Calculations with the Double-Hybrid B2PLYP Method: Analytic Second Derivatives and Benchmark Studies. *J. Chem. Theory Comput.* **2010**, *6* (7), 2115−2125.

(45) Carnimeo, I.; Cappelli, C.; Barone, V. Analytical Gradients for MP2, Double Hybrid Functionals, and TD-DFT with Polarizable Embedding Described by Fluctuating Charges. *J. Comput. Chem.* **2015**, *36* (31), 2271−2290.

(46) Barone, V.; Ceselin, G.; Fusè, M.; Tasinato, N. Accuracy Meets Interpretability for Computational Spectroscopy by Means of Hybrid and Double-Hybrid Functionals. *Front. Chem.* **2020**, *8*, 1−14.

(47) Melli, A.; Tonolo, F.; Barone, V.; Puzzarini, C. Extending the Applicability of the Semi-Experimental Approach by Means of "Template Molecule" and "Linear Regression" Models on Top of DFT Computations. *J. Phys. Chem. A* **2021**, *125* (45), 9904−9916.

(48) Goerigk, L.; Hansen, A.; Bauer, C.; Ehrlich, S.; Najibi, A.; Grimme, S. A Look at the Density Functional Theory Zoo with the Advanced GMTKN55 Database for General Main Group Thermochemistry, Kinetics and Noncovalent Interactions. *Phys. Chem. Chem. Phys.* **2017**, *19* (48), 32184−32215.

(49) Mardirossian, N.; Head-Gordon, M. Thirty Years of Density Functional Theory in Computational Chemistry: An Overview and Extensive Assessment of 200 Density Functionals. *Mol. Phys.* **2017**, *115* (19), 2315−2372.

(50) Martin, J. M. L.; Santra, G. Empirical Double-Hybrid Density Functional Theory: A 'Third Way' in Between WFT and DFT. *Isr. J. Chem.* **2020**, *60* (8−9), 787−804.

(51) Najibi, A.; Casanova-Páez, M.; Goerigk, L. Analysis of Recent BLYP- and PBE-Based Range-Separated Double-Hybrid Density Functional Approximations for Main-Group Thermochemistry, Kinetics, and Noncovalent Interactions. *J. Phys. Chem. A* **2021**, *125* (18), 4026−4035.

(52) Brémond, É.; Pérez-Jiménez, Á. J.; Sancho-García, J. C.; Adamo, C. Range-Separated Hybrid Density Functionals Made Simple. *J. Chem. Phys.* **2019**, *150* (20), 201102.

(53) Mehta, N.; Casanova-Páez, M.; Goerigk, L. Semi-Empirical or Non-Empirical Double-Hybrid Density Functionals: Which Are More Robust? *Phys. Chem. Chem. Phys.* **2018**, *20* (36), 23175−23194.

(54) Dohm, S.; Hansen, A.; Steinmetz, M.; Grimme, S.; Checinski, M. P. Comprehensive Thermochemical Benchmark Set of Realistic Closed-Shell Metal Organic Reactions. *J. Chem. Theory Comput.* **2018**, *14* (5), 2596−2608.

(55) Iron, M. A.; Janes, T. Evaluating Transition Metal Barrier Heights with the Latest Density Functional Theory Exchange−Correlation Functionals: The MOBH35 Benchmark Database. *J. Phys. Chem. A* **2019**, *123* (17), 3761−3781.

(56) Santra, G.; Martin, J. M. L. Some Observations on the Performance of the Most Recent Exchange-Correlation Functionals for the Large and Chemically Diverse GMTKN55 Benchmark. *AIP Conf. Proc.* **2019**, *2186* (2), No. 030004.

(57) Maurer, L. R.; Bursch, M.; Grimme, S.; Hansen, A. Assessing Density Functional Theory for Chemically Relevant Open-Shell Transition Metal Reactions. *J. Chem. Theory Comput.* **2021**, *17* (10), 6134−6151.

(58) Wappett, D. A.; Goerigk, L. Toward a Quantum-Chemical Benchmark Set for Enzymatically Catalyzed Reactions: Important Steps and Insights. *J. Phys. Chem. A* **2019**, *123* (32), 7057−7074.

(59) Wappett, D. A.; Goerigk, L. A Guide to Benchmarking Enzymatically Catalysed Reactions: The Importance of Accurate Reference Energies and the Chemical Environment. *Theor. Chem. Acc.* **2021**, *140* (6), 68.

(60) Zheng, J.; Zhao, Y.; Truhlar, D. G. Representative Benchmark Suites for Barrier Heights of Diverse Reaction Types and Assessment of Electronic Structure Methods for Thermochemical Kinetics. *J. Chem. Theory Comput.* **2007**, *3* (2), 569−582.

(61) Zhao, Y.; González-García, N.; Truhlar, D. G. Benchmark Database of Barrier Heights for Heavy Atom Transfer, Nucleophilic Substitution, Association, and Unimolecular Reactions and Its Use to Test Theoretical Methods. *J. Phys. Chem. A* **2005**, *109* (9), 2012−2018.

(62) Yu, L.-J.; Sarrami, F.; O'Reilly, R. J.; Karton, A. Reaction Barrier Heights for Cycloreversion of Heterocyclic Rings: An Achilles' Heel for DFT and Standard Ab Initio Procedures. *Chem. Phys.* **2015**, *458*, 1−8.

(63) Chan, B.; Simmie, J. M. Barriometry − an Enhanced Database of Accurate Barrier Heights for Gas-Phase Reactions. *Phys. Chem. Chem. Phys.* **2018**, *20* (16), 10732−10740.

(64) Goerigk, L.; Sharma, R. The INV24 Test Set: How Well Do Quantum-Chemical Methods Describe Inversion and Racemization Barriers? *Can. J. Chem.* **2016**, *94* (12), 1133−1143.

(65) Karton, A.; O'Reilly, R. J.; Radom, L. Assessment of Theoretical Procedures for Calculating Barrier Heights for a Diverse Set of Water-Catalyzed Proton-Transfer Reactions. *J. Phys. Chem. A* **2012**, *116* (16), 4211−4221.

(66) Karton, A.; O'Reilly, R. J.; Chan, B.; Radom, L. Determination of Barrier Heights for Proton Exchange in Small Water, Ammonia, and

Hydrogen Fluoride Clusters with G4(MP2)-Type, MP*n*, and SCS-MP*n* Procedures—A Caveat. *J. Chem. Theory Comput.* **2012**, *8* (9), 3128−3136.

(67) Grambow, C. A.; Pattanaik, L.; Green, W. H. Reactants, Products, and Transition States of Elementary Chemical Reactions Based on Quantum Chemistry. *Sci. Data* **2020**, *7* (1), 1−8.

(68) von Rudorff, G. F.; Heinen, S. N.; Bragato, M.; von Lilienfeld, O. A. Thousands of Reactants and Transition States for Competing E2 and S$_N$2 Reactions. *Mach. Learn. Sci. Technol.* **2020**, *1* (4), No. 045026.

(69) Prasad, V. K.; Pei, Z.; Edelmann, S.; Otero-de-la-Roza, A.; DiLabio, G. A. BH9, a New Comprehensive Benchmark Data Set for Barrier Heights and Reaction Energies: Assessment of Density Functional Approximations and Basis Set Incompleteness Potentials. *J. Chem. Theory Comput.* **2022**, *18* (1), 151−166.

(70) Prasad, V. K.; Pei, Z.; Edelmann, S.; Otero-de-la-Roza, A.; DiLabio, G. A. Correction to "BH9, a New Comprehensive Benchmark Data Set for Barrier Heights and Reaction Energies: Assessment of Density Functional Approximations and Basis Set Incompleteness Potentials. *J. Chem. Theory Comput.* **2022**, *18* (6), 4041−4044.

(71) Riplinger, C.; Neese, F. An Efficient and near Linear Scaling Pair Natural Orbital Based Local Coupled Cluster Method. *J. Chem. Phys.* **2013**, *138* (3), No. 034106.

(72) Riplinger, C.; Sandhoefer, B.; Hansen, A.; Neese, F. Natural Triple Excitations in Local Coupled Cluster Calculations with Pair Natural Orbitals. *J. Chem. Phys.* **2013**, *139* (13), 134101.

(73) Riplinger, C.; Pinski, P.; Becker, U.; Valeev, E. F.; Neese, F. Sparse Maps - A Systematic Infrastructure for Reduced-Scaling Electronic Structure Methods. II. Linear Scaling Domain Based Pair Natural Orbital Coupled Cluster Theory. *J. Chem. Phys.* **2016**, *144* (2), 024109.

(74) Saitow, M.; Becker, U.; Riplinger, C.; Valeev, E. F.; Neese, F. A New Near-Linear Scaling, Efficient and Accurate, Open-Shell Domain-Based Local Pair Natural Orbital Coupled Cluster Singles and Doubles Theory. *J. Chem. Phys.* **2017**, *146* (16), 164105.

(75) Guo, Y.; Riplinger, C.; Becker, U.; Liakos, D. G.; Minenkov, Y.; Cavallo, L.; Neese, F. Communication: An Improved Linear Scaling Perturbative Triples Correction for the Domain Based Local Pair-Natural Orbital Based Singles and Doubles Coupled Cluster Method [DLPNO-CCSD(T)]. *J. Chem. Phys.* **2018**, *148* (1), 011101.

(76) Brémond, É.; Li, H.; Pérez-Jiménez, Á. J.; Sancho-García, J. C.; Adamo, C. Tackling an Accurate Description of Molecular Reactivity with Double-Hybrid Density Functionals. *J. Chem. Phys.* **2022**, *156* (16), 161101.

(77) Neese, F. Software Update: The ORCA Program System—Version 5.0. *Wiley Interdiscip. Rev. Comput. Mol. Sci.* **2022**, *12*, e1606.

(78) Epifanovsky, E.; Gilbert, A. T. B.; Feng, X.; Lee, J.; Mao, Y.; Mardirossian, N.; Pokhilko, P.; White, A. F.; Coons, M. P.; Dempwolff, A. L.; et al. Software for the Frontiers of Quantum Chemistry: An Overview of Developments in the Q-Chem 5 Package. *J. Chem. Phys.* **2021**, *155* (8), No. 084801.

(79) Weigend, F.; Ahlrichs, R. Balanced Basis Sets of Split Valence, Triple Zeta Valence and Quadruple Zeta Valence Quality for H to Rn: Design and Assessment of Accuracy. *Phys. Chem. Chem. Phys.* **2005**, *7* (18), 3297−3305.

(80) Zheng, J.; Xu, X.; Truhlar, D. G. Minimally Augmented Karlsruhe Basis Sets. *Theor. Chem. Acc.* **2011**, *128* (3), 295−305.

(81) Hättig, C. Optimization of Auxiliary Basis Sets for RI-MP2 and RI-CC2 Calculations: Core−Valence and Quintuple-ζ Basis Sets for H to Ar and QZVPP Basis Sets for Li to Kr. *Phys. Chem. Chem. Phys.* **2005**, *7* (1), 59−66.

(82) Izsak, R.; Neese, F. An Overlap Fitted Chain of Spheres Exchange Method. *J. Chem. Phys.* **2011**, *135* (14), 144105.

(83) Dasgupta, S.; Herbert, J. M. Standard Grids for High-Precision Integration of Modern Density Functionals: SG-2 and SG-3. *J. Comput. Chem.* **2017**, *38* (12), 869−882.

(84) Mehta, N.; Fellowes, T.; White, J. M.; Goerigk, L. CHAL336 Benchmark Set: How Well Do Quantum-Chemical Methods Describe Chalcogen-Bonding Interactions? *J. Chem. Theory Comput.* **2021**, *17* (5), 2783−2806.

(85) Mardirossian, N.; Head-Gordon, M. Mapping the Genome of Meta-Generalized Gradient Approximation Density Functionals: The Search for B97M-V. *J. Chem. Phys.* **2015**, *142* (7), No. 074111.

(86) Becke, A. D. Density-Functional Thermochemistry. V. Systematic Optimization of Exchange-Correlation Functionals. *J. Chem. Phys.* **1997**, *107* (20), 8554−8560.

(87) Grimme, S.; Ehrlich, S.; Goerigk, L. Effect of the Damping Function in Dispersion Corrected Density Functional Theory. *J. Comput. Chem.* **2011**, *32* (7), 1456−1465.

(88) Hamprecht, F. A.; Cohen, A. J.; Tozer, D. J.; Handy, N. C. Development and Assessment of New Exchange-Correlation Functionals. *J. Chem. Phys.* **1998**, *109* (15), 6264−6271.

(89) Boese, A. D.; Martin, J. M. L. Development of Density Functionals for Thermochemical Kinetics. *J. Chem. Phys.* **2004**, *121* (8), 3405−3416.

(90) Grimme, S.; Antony, J.; Ehrlich, S.; Krieg, H. A Consistent and Accurate Ab Initio Parametrization of Density Functional Dispersion Correction (DFT-D) for the 94 Elements H-Pu. *J. Chem. Phys.* **2010**, *132* (15), 154104.

(91) Chai, J.-D.; Head-Gordon, M. Long-Range Corrected Hybrid Density Functionals with Damped Atom−Atom Dispersion Corrections. *Phys. Chem. Chem. Phys.* **2008**, *10* (44), 6615.

(92) Chai, J.-D.; Head-Gordon, M. Long-Range Corrected Double-Hybrid Density Functionals. *J. Chem. Phys.* **2009**, *131* (17), 174105.

(93) Perdew, J. P.; Burke, K.; Ernzerhof, M. Generalized Gradient Approximation Made Simple. *Phys. Rev. Lett.* **1996**, *77* (18), 3865−3868.

(94) Perdew, J. P.; Burke, K.; Ernzerhof, M. Errata:Generalized Gradient Approximation Made Simple [Phys. Rev. Lett. 77, 3865 (1996)]. *Phys. Rev. Lett.* **1997**, *78* (7), 1396−1396.

(95) Chai, J. Da; Mao, S. P. Seeking for Reliable Double-Hybrid Density Functionals without Fitting Parameters: The PBE0−2 Functional. *Chem. Phys. Lett.* **2012**, *538*, 121−125.

(96) Goerigk, L.; Grimme, S. Double-Hybrid Density Functionals. *Wiley Interdiscip. Rev. Comput. Mol. Sci.* **2014**, *4* (6), 576−600.

(97) Alipour, M. Seeking for Spin-Opposite-Scaled Double-Hybrid Models Free of Fitted Parameters. *J. Phys. Chem. A* **2016**, *120* (20), 3726−3730.

(98) Brémond, E.; Adamo, C. Seeking for Parameter-Free Double-Hybrid Functionals: The PBE0-DH Model. *J. Chem. Phys.* **2011**, *135* (2), No. 024106.

(99) Sancho-García, J. C.; Brémond, É.; Savarese, M.; Pérez-Jiménez, A. J.; Adamo, C. Partnering Dispersion Corrections with Modern Parameter-Free Double-Hybrid Density Functionals. *Phys. Chem. Chem. Phys.* **2017**, *19* (21), 13481−13487.

(100) Brémond, É.; Savarese, M.; Sancho-García, J. C.; Pérez-Jiménez, Á. J.; Adamo, C. Quadratic Integrand Double-Hybrid Made Spin-Component-Scaled. *J. Chem. Phys.* **2016**, *144* (12), 124104.

(101) Becke, A. D. Density-Functional Exchange-Energy Approximation with Correct Asymptotic Behavior. *Phys. Rev. A* **1988**, *38* (6), 3098−3100.

(102) Lee, C.; Yang, W.; Parr, R. G. Development of the Colle-Salvetti Correlation-Energy Formula into a Functional of the Electron Density. *Phys. Rev. B* **1988**, *37* (2), 785−789.

(103) Becke, A. D. Density-functional Thermochemistry. III. The Role of Exact Exchange. *J. Chem. Phys.* **1993**, *98* (7), 5648−5652.

(104) Stephens, P. J.; Devlin, F. J.; Chabalowski, C. F.; Frisch, M. J. Ab Initio Calculation of Vibrational Absorption and Circular Dichroism Spectra Using Density Functional Force Fields. *J. Phys. Chem.* **1994**, *98* (45), 11623−11627.

(105) Becke, A. D. A New Mixing of Hartree−Fock and Local Density-functional Theories. *J. Chem. Phys.* **1993**, *98* (2), 1372−1377.

(106) Grimme, S. Semiempirical Hybrid Density Functional with Perturbative Second-Order Correlation. *J. Chem. Phys.* **2006**, *124* (3), No. 034108.

(107) Karton, A.; Tarnopolsky, A.; Lamère, J.-F.; Schatz, G. C.; Martin, J. M. L. Highly Accurate First-Principles Benchmark Data Sets for the Parametrization and Validation of Density Functional and Other Approximate Methods. Derivation of a Robust, Generally Applicable,

Double-Hybrid Functional for Thermochemistry and Thermochemical. *J. Phys. Chem. A* **2008**, *112* (50), 12868−12886.

(108) Kozuch, S.; Martin, J. M. L. Spin-Component-Scaled Double Hybrids: An Extensive Search for the Best Fifth-Rung Functionals Blending DFT and Perturbation Theory. *J. Comput. Chem.* **2013**, *34* (27), 2327−2344.

(109) Santra, G.; Sylvetsky, N.; Martin, J. M. L. Minimally Empirical Double-Hybrid Functionals Trained against the GMTKN55 Database: revDSD-PBEP86-D4, revDOD-PBE-D4, and DOD-SCAN-D4. *J. Phys. Chem. A* **2019**, *123* (24), 5129−5143.

(110) Perdew, J. P.; Ernzerhof, M.; Burke, K. Rationale for Mixing Exact Exchange with Density Functional Approximations. *J. Chem. Phys.* **1996**, *105* (22), 9982−9985.

(111) Adamo, C.; Barone, V. Toward Reliable Density Functional Methods without Adjustable Parameters: The PBE0 Model. *J. Chem. Phys.* **1999**, *110* (13), 6158−6170.

(112) Furness, J. W.; Kaplan, A. D.; Ning, J.; Perdew, J. P.; Sun, J. Accurate and Numerically Efficient r^2SCAN Meta-Generalized Gradient Approximation. *J. Phys. Chem. Lett.* **2020**, *11* (19), 8208−8215.

(113) Furness, J. W.; Kaplan, A. D.; Ning, J.; Perdew, J. P.; Sun, J. Correction to "Accurate and Numerically Efficient r^2SCAN Meta-Generalized Gradient Approximation. *J. Phys. Chem. Lett.* **2020**, *11* (21), 9248−9248.

(114) Bursch, M.; Neugebauer, H.; Ehlert, S.; Grimme, S. Dispersion Corrected r^2SCAN Based Global Hybrid Functionals:r^2SCANh, r^2SCAN0, and r^2SCAN50. *J. Chem. Phys.* **2022**, *156* (13), 134105.

(115) Tao, J.; Perdew, J. P.; Staroverov, V. N.; Scuseria, G. E. Climbing the Density Functional Ladder: Nonempirical Meta−Generalized Gradient Approximation Designed for Molecules and Solids. *Phys. Rev. Lett.* **2003**, *91* (14), 146401.

(116) Staroverov, V. N.; Scuseria, G. E.; Tao, J.; Perdew, J. P. Comparative Assessment of a New Nonempirical Density Functional: Molecules and Hydrogen-Bonded Complexes. *J. Chem. Phys.* **2003**, *119* (23), 12129−12137.

(117) Grimme, S. Accurate Calculation of the Heats of Formation for Large Main Group Compounds with Spin-Component Scaled MP2Methods. *J. Phys. Chem. A* **2005**, *109* (13), 3067−3077.

(118) Kim, M.-C.; Sim, E.; Burke, K. Understanding and Reducing Errors in Density Functional Calculations. *Phys. Rev. Lett.* **2012**, *111* (7), 1−5.

(119) Santra, G.; Martin, J. M. L. What Types of Chemical Problems Benefit from Density-Corrected DFT? A Probe Using an Extensive and Chemically Diverse Test Suite. *J. Chem. Theory Comput.* **2021**, *17* (3), 1368−1379.

(120) Caldeweyher, E.; Ehlert, S.; Hansen, A.; Neugebauer, H.; Spicher, S.; Bannwarth, C.; Grimme, S. A Generally Applicable Atomic-Charge Dependent London Dispersion Correction. *J. Chem. Phys.* **2019**, *150* (15), 154122.

(121) Kim, Y.; Song, S.; Sim, E.; Burke, K. Halogen and Chalcogen Binding Dominated by Density-Driven Errors. *J. Phys. Chem. Lett.* **2019**, *10* (2), 295−301.

(122) Wasserman, A.; Nafziger, J.; Jiang, K.; Kim, M.-C.; Sim, E.; Burke, K. The Importance of Being Inconsistent. *Annu. Rev. Phys. Chem.* **2017**, *68* (1), 555−581.

(123) Santra, G.; Martin, J. M. L. Pure and Hybrid SCAN, rSCAN, and r^2SCAN: Which One Is Preferred in KS- and HF-DFT Calculations, and How Does D4 Dispersion Correction Affect This Ranking? *Molecules* **2022**, *27* (1), 141.